ANALYSIS OF RETINAL FUNDUS IMAGES FOR GLAUCOMA SCREENING

A Dissertation submitted in fulfillment of the requirements for the Degree
Of

MASTER OF ENGINEERING
In
Electronic Instrumentation & Control Engineering

Submitted by

Jiwanpreet Kaur Virk
801351006

Under the Guidance of
Mooninder Singh
Assistant Professor, EIED

2015

Electrical and Instrumentation Engineering Department
Thapar University, Patiala
(Declared as Deemed-to-be-University u/s 3 of the UGC Act., 1956)
Post Bag No. 32, Patiala – 147004
Punjab (India)

DECLARATION

I hereby certify that the work which is presented in dissertation entitled, "**Analysis of Retinal Fundus Images for Glaucoma Screening**" in partial fulfillment of the requirements for the award of the degree of **Master of Engineering** in **Electronics (Instrumentation & Control)**, submitted to Electrical & Instrumentation Engineering Department of Thapar University, Patiala is as authentic record of my own work carried under the supervision of **Mr. Mooninder Singh**, Assistant Professor, Electrical and Instrumentation Engineering Department, Thapar University, Patiala, Punjab. It refers others researcher's work which are duly listed in the reference section. The matter contained in this dissertation has not been submitted, neither in part nor in full to any other degree to any other university or institute except as reported in text and references.

Place: Patiala

Date: 15/07/2015

Jiwanpreet
(Jiwanpreet Kaur Virk)

Roll No: 801351006

It is certified that the above statement made by the student is correct to the best of my knowledge and belief.

Mooninder Singh
(Mr. Mooninder Singh)

Assistant Professor

Electrical & Instrumentation Engineering Department

Thapar University, Patiala

Date: 15/07/2015

Countersigned by:

Head

Electrical & Instrumentation Engineering Department

Thapar University, Patiala

Dean (Academic Affairs)

Thapar University, Patiala

ACKNOWLEDGEMENT

First of all, I would like to express my gratitude to **Mr. Mooninder Singh, Assistant Professor,** Electrical and Instrumentation Engineering Department (EIED), Thapar University, Patiala for his patient guidance and support. I am truly very fortunate to have the opportunity to work with him. I found his guidance to be extremely valuable. I am also grateful to **Dr. Mandeep Singh, Associate Professor,** Electrical and Instrumentation Engineering Department (EIED), Thapar University for his valuable guidance.

I am also thankful to our **HEAD OF THE DEPARTMENT, Dr. Ravinder Agarwal** as well as **PG Coordinator, Mr. Nirbhowjap Singh, Assistant Professor**, Electrical and Instrumentation Engineering Department.

I am extremely thankful to **Dr. Animesh Jindal**, Vitreo-Retina Surgeon, G. S. Randhawa Eye Hospital, Patiala for his helpful guidance the time he devoted on me to help me to understand the medical concepts more clearly.

I would like to thank entire faculty and staff of Electrical and Instrumentation Engineering Department and then my friends who devoted their valuable time and helped me in all possible ways towards successful completion of this work. I thank all those who have contributed directly or indirectly to this work.

Lastly, I would also like to thank my parents for their years of unyielding love and encourage. They have always wanted the best for me and I admire their determination and sacrifice.

Jiwanpreet

JIWANPREET KAUR VIRK

M.E. (EICE) 2nd Year

801351006

Date: 15/07/2015

Place: Patiala

TABLE OF CONTENTS

LIST OF TABLES

LIST OF FIGURES

LIST OF ABBREVIATIONS

ACM- Active Contour Model

ANFIS- Adaptive Neuro Fuzzy Inference System

ANN- Artificial Neural Network

ASM- Active Shape Model

CDR- Cup-To-Disc Ratio

DRIVE- Digital Retinal Images for Vessel Extraction

FCM- Fuzzy C-Mean Clustering

FDR - False Discovery Rate

Fig- Figure

FN- False Negative

FNR - False Negative Rate

FP- False Positive

FPR - False Positive rate

IOP- Intra-Ocular Pressure

ISNT- Inferior Superior Nasal Temporal

LDA- Linear Discriminant Analysis

NPV - Negative Predictive Value

NRRA - Neuro-Retinal Rim Area

OC- Optic Cup

OD- Optic Disc

OHN- Optic Head Normalization

ONH- Optic Nerve Head

PCA- Principal Component Analysis

PPV - Positive Predictive Value

RGB- Red Green Blue

RNF- Retinal Nerve Fiber

SE- Structuring Element

STARE- Structured Analysis of Retina

TN- True Negative

TP- True Positive

ABSTRACT

The processing of a Fundus image using different computer aided techniques are used for the extraction of its distinct features for the diagnosis and screening of the deformities related to human body. The eye's fundus is the only part of the human body where the microcirculation is be observed directly. Several medical signs that can be detected from funduscopy include hemorrhages, blood vessel abnormalities; exudates and pigmentation. The Optic Disc (OD), Optic Cup (OC), Neuro-Retinal Rim Area (NRRA), ISNT (Inferior-Superior-Nasal-Temporal) Quadrants are the main contrasting features of a Fundus image. There are some diseases which do not show any symptoms at early stages but if not detected earlier they may lead to severe consequences. One such disease is Glaucoma. If not detected, diagnosed and cured at prior stages it may lead to complete vision loss. The shape, size and orientation of the Fundus image features are altered in a pathological condition that can be observed during early stages. These changes can be detected and identified by using the image processing techniques and hence preventive measures can be taken to avoid any further damage. The methodology has been applied on a database acquired from a local physician. In this dissertation work, the size and shape of the Optic Disc and Cup are used as the major features for calculating the Cup-to-Disc Ratio which classifies the image samples as normal or suspicious for Glaucoma. The methodology proposed extracts out the Optic Disc and Cup from a color retinal Fundus image. The value of Cup-to-Disc Ratio is calculated by estimating the diameters of the extracted Disc and Cup. This ratio then screens the images for Glaucoma. The ratios obtained are compared with the gold standard values and the algorithm showed a detection rate of 80% and classification accuracy of 95%, sensitivity and specificity of 100% and 91% respectively.

CHAPTER 1
INTRODUCTION

1.1 Overview

Glaucoma is a term referring to a group of eye disorders that leads to optic nerve damage which, in most cases, is associated with an elevated fluid pressure in the eye i.e. Intra-Ocular Pressure (IOP). Most of these diseases give rise to elevated pressure within the eye. The Intra-Ocular Pressure (IOP) is measured in millimeters of Hg and ranges from 10-21 mm Hg in normal subjects by a tonometer [1, 2]. An elevated eye pressure is one of the major risk factors for glaucoma and can be used for its screening. In Glaucoma, higher eye pressure damages the delicate nerve fibers and blood vessels and finally the optic nerve as shown in Figure 1.1. In front of the eye there is a small space called the „anterior chamber" and a clear fluid flows through it and nourishes the nearby tissues and the trabecular meshwork. This very fluid is the aqueous humor which is basically a transparent fluid consisting of low protein concentrations. It is discharged by the ciliary bodies (in the posterior chamber a space between the iris and the lens). The fluid after being secreted then flows through the pupil into the anterior chamber between the iris and the cornea and goes in episcleral vein as shown in Figure 1.2. From here it drains through a sponge like structure located at the base of the iris called the trabecular meshwork and finally exits from the eye. In a healthy eye, the rate of secretion is equivalent to the rate of drainage. But in people with Glaucoma this drainage channel is blocked since it does not flow out it starts accumulating in the chamber and this increase the pressure in the chamber as well as within the eye. The pressure then pushes the lens back and presses on the vitreous humor or the body which in turn compresses and damages the blood vessels and the nerve fibers running at the back of the eye and finally the optic nerve, which transmits visual information from the retina to the brain. These injured blood vessels leads to the patches of vision loss and if left untreated may lead to total blindness [2].

Elevated eye pressure signifies that the subject is at risk, but does not mean that she has glaucoma. A person is glaucomatous only if the optic nerve is harmed. If someone has an elevated IOP but unharmed optic nerve, she is not considered glaucomatous but is at risk.

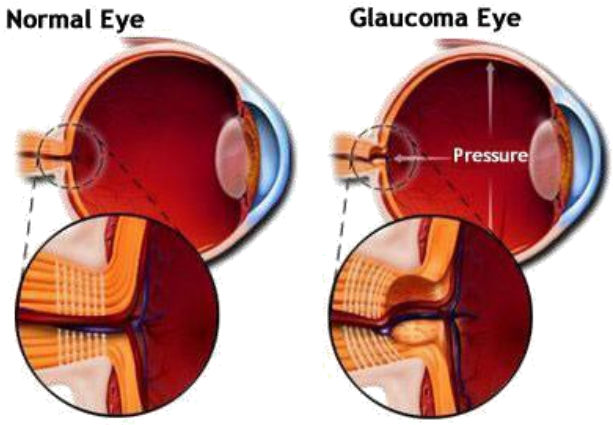

Figure 1.1: Effect of pressure on Optic Nerve [3]

Also not everyone with increased IOP will have glaucoma. A certain level of eye pressure may be high for one but normal for another. Glaucoma can also develop without an elevated IOP. This is another form of glaucoma called normal-tension glaucoma.

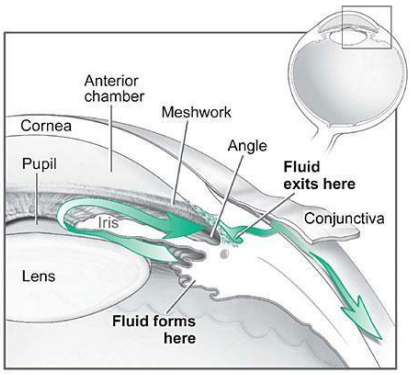

Figure 1.2: Aqueous Fluid Pathway [4]

1.2 Types of Glaucoma

There are different types of glaucoma namely:

*Open Angle/ Chronic Glaucoma***:** It is caused by the partial blockage of the drainage canal. The angle between cornea and iris is open meaning the entrance to the drain is clear, but the aqueous humor flow is somewhat slow. The pressure in the eye builds up gradually over a long period of time. Also the symptoms appear gradually starting with peripheral vision loss and may go unnoticed until the central vision is affected. The progression can be stopped with the medical

treatments but the part of vision that is already lost cannot be restored, that is why the early detection of glaucoma is very important.

*Acute Angle Closure Glaucoma***:** It is caused by sudden and complete blockage of the aqueous humor drainage. The pressure within the eye arises rapidly and may lead to total vision loss quickly. The anatomical features of eye like narrow drainage angle, shallow anterior chamber, thin and droopy iris make it easier to develop this type of glaucoma. Typically this happens when the pupil is dilated and the lens is stuck to the back of the iris. This prevents the aqueous humor form flowing through the pupil into the anterior chamber. This results in the accumulation of the fluid in the posterior chamber which further presses the iris causing it to bulge outwards and block the drainage angle completely. This is basically a medical emergency and requires immediate attention. Usually, laser surgery and medicines can clear the blockage, lower eye pressure, and protect vision [2].

*Normal Tension Glaucoma***:** It is an eye disorder that shows all the features of traditional glaucoma except the elevated IOP. It is in many cases associated with issues of blood circulation. It has symptoms like increased optic nerve head (ONH) excavation and thinning of the retinal fiber layer, while the patient has an IOP that is regarded as normal.

*Ocular Hypertension***:** It is a term signifying the presence of IOP in the absence of optic nerve damage or even visual loss. The normal range of IOP is between 10 - 21 mm of Hg.

*Secondary Glaucoma***:** This glaucoma results from another eye disease. Like, if the patient had an eye injury or who is on prolonged steroid therapy or who has a tumor may flourish secondary glaucoma.

*Congenital Glaucoma***:** It is an infrequent type of glaucoma that evolves in infants and young children and may be inherited. Conventional surgery is the suggested treatment as medicines are not effective and may cause serious side effects in infants [5].

1.3 Causes of Glaucoma

General causes leading to Glaucoma:

- Old age - People of age above 60 are more prone to develop glaucoma

- Other illnesses and Conditions - People with diabetes have a higher chance of developing glaucoma
- Eye injuries - Eye injuries are linked to a higher glaucoma risk. Retinal detachment, eye tumors and inflammations can also lead to glaucoma
- Eye surgery – patients who underwent eye surgery have a higher risk of glaucoma
- Myopia - people with myopia also have a risk of glaucoma
- Corticosteroids – These are a class of chemical drugs that constitutes the steroid hormones. Patients on prolonged use corticosteroids have a higher risk of developing glaucoma
- Migraine and peripheral vasospasm have also been identified as risk factors for glaucomatous optic nerve damage [5]

1.4 Diagnosis of Glaucoma

Glaucomatous diagnosis is based on the patient‟s family medical and genetic history, thinner corneas, elevated Intra Ocular Pressure and manual assessment of the Optic Nerve Head from the color fundus images [6]. It is basically denoted by the changes in the eye ground i.e. the region of the Optic Nerve Head (ONH) and it is evaluated by analysis of special optic images known as Fundus images acquired with the help of a special instrument called the Ophthalmoscope. This fundus image consists of a few notable features, as shown in Figure 1.3,that are evaluated to conclude and classify it as normal or suspicious (Glaucomatous).

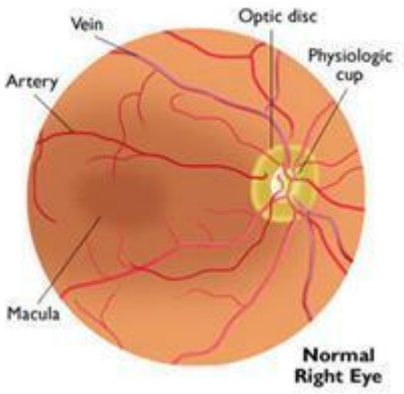

Figure 1.3: Normal Fundus [7]

Optic disc (OD) is the most vivid feature in a normal retinal fundus image and it has an elliptical shape. It appears as a bright orange-pink ellipse with a pale centre. Orange-pink appearance signifies a healthy neuro-retinal tissue. Due to the pathologies, the orange-pink color moderately disappears and appears pale. Blood vessels are emerging out from the Optic Disc (OD). The pale centre is devoid of neuro-retinal tissue and is known as the Optic Cup (OC). The vertical size of this cup can be estimated corresponding to the disc as a whole and extended as a cup-to-disc ratio (CDR). The CDR marks the proportion of the disc encompassed by the cup and is widely accepted figure for the screening of glaucoma. For a normal eye it is acceptable from 0.3 to 0.5. As the neuro-retinal degeneration precedes the ratio increases and at the value of 0.8 the vision is completely lost. Figure 1.4(a) and (b) shows a healthy Optic disc with normal CDR and unhealthy Optic Disc with abnormal CDR value respectively. The CDR value thus may be used to screen glaucomatous cases.

For detecting Glaucoma we use CDR primarily for the screening purpose. The subjects with a CDR value higher than 0.5 are considered as suspicious and need further confirmatory tests. The sample with a CDR value lesser than 0.5 is surely not glaucomatous and this does not require any further investigation. For confirming Glaucoma changes in Neuro-Retinal Rim (NRR) and ISNT Quadrants are studied.

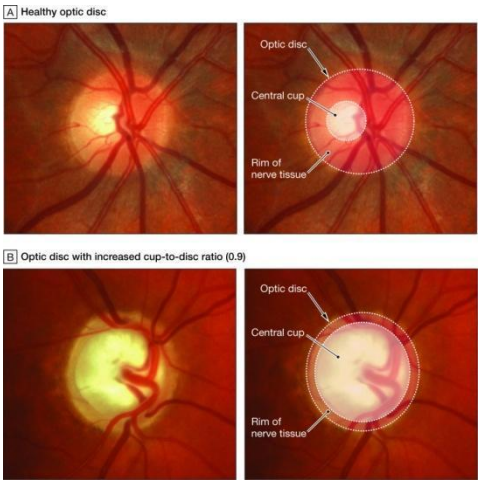

Figure 1.4: (a) Healthy Optic Disc (b) Unhealthy Optic Disc [8]

Neuro-Retinal Rim (NRR) Area is the region between the boundary of the disc and the physiological Cup as shown in Figure 1.4. The NRR is normally thickest in the inferior part;

followed by the superior, nasal and the temporal. This is referred to as the "ISNT" rule which is observed in the normal cases shown in Figure 1.5. Any change in this pattern is suspicious like if the inferior rim or part is thinner as compared to the superior, it could suggest pathology. The temporal rim is thinnest for normal cases. In glaucomatous cases, the ratio of the area covered by the rim in superior and inferior region reduces and becomes thin as compared to the area covered by the rim in nasal and temporal region.

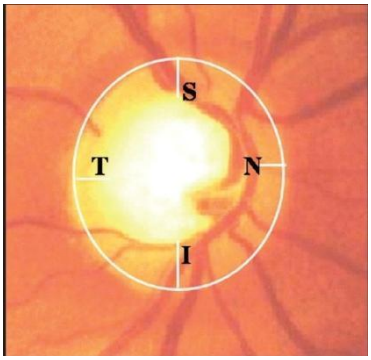

Figure 1.5: ISNT rule [9]

The glaucomatous changes observed in the color retinal fundus may include:

(i) expansion of the cavity (Cup),

(ii) the changes in the appearance of Optic Disc (OD)

(iii) disc hemorrhage,

(iv) thinning of the neuro-retinal rim area,

(v) unevenness of the cup between left and right eye,

(vi) loss of retinal nerve fibers

1.5 Outline of Dissertation

This dissertation consists of 7 chapters that have been briefed below to get an overview of the work done.

Chapter 1 is Introduction. It basically provides an introduction to the disease Glaucoma. Different types of the disease, causes that lead to Glaucoma and its diagnosis have been discussed. It explains different features of the Fundus image. All the features that are altered by the presence of the disease have been discussed.

Chapter 2 is Literature survey. This chapter highlights the various researches that have been carried out in the field of retinal imaging for the extraction of various features of a Fundus image using image processing. It also compares the different methods followed by the researchers.

Chapter 3 is the Problem Definition. It outlines the aim of the dissertation.

Chapter 4 is the Proposed Solution. This chapter frames the work carried out. It also briefs the steps taken up to evaluate the performance of the algorithm proposed.

Chapter 5 is the Proposed Methodology. It explains the various steps involved in the methodology. The image samples that have been processed upon using the proposed methodology are acquired from a local physician. The images have been applied with image processing techniques. The algorithm has been applied on a total of 50 image samples.

Chapter 6 is Results. This chapter highlights the results of the image processing techniques that have been applied on the sample images. It holds the values of diameters of the Optic Disc and Cup and also their Cup-to-Disc Ratios. It mentions the results of Student‟s t-test applied. The results of the confusion matrix plotted have also been shown.

Chapter 7 is Conclusion and Future scope. The conclusion of this research has been mentioned in this chapter. It also highlights the improvements and the future work that can be done.

CHAPTER 2
LITERATURE REVIEW

Huiqi Li *et al.* (2003) presented a new approach to extract the main features from a color fundus image. Optic disc was first localized by the principal component analysis (PCA) and then its shape was segmented by an active shape model (ASM) [10]. PCA was proposed to localize the optic disc. The procedure was performed on the intensity image. The steps in the localization were:

- The candidate regions were determined and PCA is employed.
- A sub-image around the disc was cropped to obtain a training image.
- An active shape model (ASM) was proposed to detect the disc boundary.

James Lowell *et al.* (2004) localized and segmented the Optic Nerve Head (ONH) from the low resolution retinal fundus images by using template matching for the disc localization followed by a deformable contour model [11].

Kevin Noronha *et al.* (2006) proposed methods to detect main features of the retinal fundus image including Optic Disc, blood vessels, and exudates [12]. Hough Transform has been used in order to find the centre of the disc and then finally its boundary. Blood vessels have been highlighted, detected and removed by using the bottom hat transformation and the morphological techniques.

The method by Atef Z. Ghalwash (2007) *et al.* included normalizing luminosity and the contrast throughout the image by using illumination equalization along with adaptive histogram equalization methods [13]. The disc detection algorithm was dependent on matching the expected directional order of the retinal blood vessels. A simple matched filter was presented to roughly match or map the direction of the vessels in the Optic Disc (OD) territory. The retinal vessels were firstly segmented using a standard Gaussian matched filter. Ultimately, a vessel direction map of the segmented retinal vessels was obtained using the same segmentation algorithm.

J. Liu *et al.* (2008) to extract the optic disc from a retinal fundus image used a variational-level-set method [14]. In case of the optic cup, two methods of color intensity with threshold level set were applied. The results signified potential applicability of these methods for automated screening for early recognition of glaucoma. Variational level-set proceeded to extract the optic disc. The extracted contours were smoothened by using direct ellipse fitting to remove the noise in the extracted boundary. The CDR was then calculated by using the extracted cup and disc dimensions.

S. Sekhar (2008) *et al.* described a novel method to localize the optic disc. The proposed methodology consists of two stages: First step, an elliptical or circular region of interest was extracted by first isolating the brightest region in the image by using of morphological processing, and, Second step, the Hough transform was applied to detect the main circular attribute within the region of interest [15].The boundary of the disc and its center were extracted out by applying the Hough transform to the morphologically operated image. The total number of edge pixels and also the number of radii used were reduced by applying Hough transform only as the computational complexities of Hough transform is completely dependent on the total number of edge pixels and the number of radii to be mapped.

Radim Kolář *et al.* (2008) described a method for glaucoma detection based on fractal dimensions followed by its classification [16]. Two methods for estimating fractal dimensions, which give a different image or tissue description, were proposed. The retinal images were used in which the areas comprising of retinal nerve fibers are examined. The proposed method showed that fractal dimensions can be employed as features for nerve fibers loss detection, which indicates a glaucomatous eye. They proposed new features for Retinal Nerve Fiber (RNF) identification applied to the texture generated by RNF layer.

G.B. Kande *et al.* (2008) used different approaches for the segmentation and detection of optic disc [17]. The Optic Disc centre is approximated by locating a point with maximum local variance and the disc boundary is detected by using geometric active contour.

X. Zhu *et al.* (2008) keeping in track the properties of the disc, used different filter methods like sobel or canny edge detectors to detect the edges and the circles using the Hough Transform [18]. The Hough Transform provides us with the centre of the disc as well as its radius and hence finally approximates the boundary or the margin of the disc. The methodology was tested on the DRIVE database.

G.B. Kande (2009) *et al.* applied stepwise preprocessing technique by converting the image into HIS (Hue Saturation Intensity) space followed by a local contrast enhancement method and a median filter which reduces the noise level of the image [19]. The optic disc boundary detection involved the use of color morphology and geometric active contour method with variational formulation.

Ahmed W. Reza *et al.* (2009) first applied an averaging filter to the original image to blend the small objects with lower intensity variations into the background itself leaving the objects of interest unchanged followed by the contrast adjustment of the extracted green channel image to make the brighter object features distinguishable from the background. The proposed algorithm used green component of the image and used preprocessing steps followed by image processing techniques such as morphological operations, maxima operator, minima imposition, and the watershed transformation [20]. The methodology was evaluated using the images of STARE and DRIVE databases by using fixed and variable thresholds.

Jagadish Nayak *et al.* (2009) presented a novel method for glaucoma detection using digital fundus images [21]. The RGB components of the images were analyzed and RED and GREEN image components were extracted out for disc and cup respectively. *First* morphological operations were applied on both the red and green components of the image. *Second,* the standard deviation as well as the threshold values for separating out the disc and the cup from the red and green images was evaluated. *Third,* Using the evaluated threshold values the red and green images were converted to binary images to obtain the disc and cup.

S. Ravishankar *et al.* (2009) presented a different methodology for the localization of different features from a fundus retinal image [22]. The OD is detected by first detecting and then

removing the blood vessels so that the boundary of the disc becomes clear. Different morphological operators have been applied for the feature detection as well.

Jörg Meier *et al.* (2010) used illumination correction, vessel removal and Optic Head Normalization (OHN) as a part of pre processing of the fundus image [23]. The illumination correction method subtracts the retinal background from the original image to get a uniformly illuminated fundus image. The estimation of the background was done by average intensity filtering. The vessel structures situated in the eye ground were removed by using segmentation and in-painting of the detected vessel branch. Also OHN template-matching, the convergence of the vessel tree or intensity assumptions were applied for OHN normalization.

Rudiger Bock *et al*. (2010) segmented blood vessels to obtain a "vessel-free" image. Also images were scaled to a uniform size of 128 × 128 pixels [24]. Different types of features (pixel intensity values, textures and parameters of a histogram model) were examined. Pixel intensity values were taken as a high dimensional feature and used principal component analysis (PCA) and linear discriminant analysis (LDA). Also the other structural changes resulted by glaucoma a set of Gabor filter banks were applied on preprocessed images. Histograms were also applied to summarize the data in the image. The change in the CDR values shows intensity shifts in the histograms models.

Chisako Muramatsu *et al.* (2010) compared three different methods of active contour model (ACM), artificial neural network (ANN), and fuzzy c-mean (FCM) clustering for the detection and extraction of the optic disc [25]. The results of each of them were evaluated using different databases from different camera systems.

Disc detection by ACM: The determination of the optic disc regions was based on the active contour modeling. In this, the expected disc boundaries were searched in spiral directions from the center of the region of interest.

Disc detection by pixel classification method: Two kinds of pixel classification techniques were investigated: FCM and ANN.

In ***FCM***, the cluster center and the membership degree was updated in every iteration. The algorithm was trained to classify the pixels into 2 to 4 clusters, and a resulting cluster that

comprised of the center pixel of the ROI regarded as the disc cluster. After applying the morphological opening, an isolated area in the center of the ROI was referred to as the disc region.

The ***ANN*** was trained with the input data and the clinical data determined by ophthalmologist. The count of the hidden units was varied corresponding to the number of units at the input. The count of output units was set corresponding to the probability of a pixel whether belonging to the disc and background or to the disc. Depending on the number of outputs, some number of pixels per group were randomly drawn or selected from each case and enrolled for training. If the output corresponding to the disc probability has the highest value, these pixels were then classified as a part of the disc region. After opening it morphologically, the isolated region in the center of the ROI was referred to as the final disc area.

Arturo Aquino *et al.* (2010) presented a template-based method which used morphological and edge detection techniques followed by Circular Hough Transform to detect disc boundary approximation [26]. It required a pixel located within the optic disc as the initial information. Firstly, a disc containing image was extracted from the fundus image from which an OD pixel and its neighboring area was selected. For this purpose, an Optic Disc (OD) location method was used. The Optic Disc (OD) boundary was extracted out in parallel from both the channels, red and green, of this sub-image by use of morphological and edge detection methods. Both the boundaries were estimated by using Circular Hough Transform.

D.W.K. Wong *et al.* (2010) presented a supervised learning scheme way out for the extraction of the optic disc [27]. This method used the pixel and local neighborhood features for the segmentation. The Support Vector Machine is the classification method used to classify the subjects.

Ahmed E. Mahfouz *et al.* (2010) proposed a faster method of segmentation of the disc [28]. It works on the projections of the image that encodes the x and the y coordinates of the disc. The resulting projections then estimate the disc boundary.

P.C. Siddalingaswamy *et al.* (2010) presented an automated computer aided algorithm for the detection of several features of a retinal fundus image including the optic disc, fovea, blood vessels and exudates [29]. Once the disc is detected, the diameter of the disc and its centre are used to detect the location of other features.

Madhusudan Mishra *et al.* (2011) used active contour method to find the CDR from the fundus images to deduce the pathological procession of glaucoma [30]. Firstly, the images were given illumination correction, after the pre-processing the blood vessels were removed from the image as they were hardly affected by the glaucoma and hence does not play any part in detecting it. And then finally the Cup and the Disc were detected by using multi thresholding and the active contour method. The cup was assigned with a higher threshold value in comparison to the disc. The method was based on the prominence of a curve around the object which is to be detected. Then the cup to disc ratio was calculated by mathematically taking the ratio of the dimensions of the cup to the disc.

A.W. Reza *et al.* (2011) used a methodology for the extraction of the Optic disc along with cotton wool spots and exudates [31]. These features were extracted using marker-controlled watershed segmentation. As the pre-processing steps, average filtering and contrast adjustment has also been used.

Fengshou Yin *et al.* (2011) presented a method dependent on the edge detection, statistical deformable technique and the Circular Hough transform for the segmentation of the disc from the color retinal fundus image [32].

Jun Cheng *et al.* (2011) segmented the optic disc by using papillary atrophy elimination. These eliminations are done using elliptical Hough Transform and edge filtering [33].

A Dehgani *et al.* (2011) proposed a novel method for the segmentation the optic disc [34]. To detect the optic disc boundary, after the removal of the blood vessels, the centre of the disc is estimated which makes the segmentation of the disc even easier.

M. Esmaeili *et al.* (2012) presented a new disc detection method build on the DCUT and level set method [35]. Firstly the bright lesions are extracted using the DCUT and the variations in the curve-let coefficients. The detected bright lesions distinguish the optic disc and the other features in the retinal fundus image.

S. Kavitha *et al.* (2012) proposed a computer aided system for automated detection of glaucoma from fundus images [36]. Detection of Glaucoma involved the measurement of the size and the shape of the Optic cup as well as Neuroretinal rim. The cup and disc areas differ in color, known as pallor. The technique was based on this pallor using K means clustering proposed to differentiate between the cup- to- disc boundary. Along with the shape based features, textural features were also extracted. The set of features selected by the Genetic algorithm were fed as input to the Adaptive Neuro Fuzzy Inference System (ANFIS) for classification.

H. Yu *et al.* (2012) used template matching to locate the Optic disc candidates [37]. Template matching is performed to basically adapt the different image resolutions. Further the blood vessel pattern is used to determine the disc location. Different morphological operations have been used to remove the blood vessels and other bright speckles or regions other than the disc.

M.H.S.P. Kumara *et al.* (2013) removed the optic disc from the fundus image by using the active contour model [38]. The methodology prevailed by first estimating the disc boundary using Circular Hough Transform, edge detection and morphology and then finally applying the active contour model resulting in the disc boundary.

Fauzia Khan *et al.* (2013) proposed image processing techniques for the early detection and diagnosis of glaucoma [39]. The Optic Disc and Cup were detected by first extracting the V plane from HSV image and then converted to gray scale image. The mean value of the gray scale image was calculated and set as threshold for binary image. For the cup, green plane was taken up and converted to gray scale image. Threshold value for the cup varies as there are gradual changes in the cup color due to which boundary of cup is not clear.

Preeti *et al.* (2013) discussed various image processing methods that has been used in the early diagnosis and evaluation of various eye diseases including Glaucoma [40]. These included Enhancement, Classification, Fusion, Segmentation, Registration, Pattern matching, Morphology, Statistical measurements, Feature extraction and Analysis.

Jun Cheng *et al.* (2013) employed the super pixel classification methodology to segment out the optic disc and cup from the fundus image [41]. To segment the disc, histogram and centre statistics are used to classify the pixels. Further to extract the cup out, along with the centre stats and histograms the local information about the cup is also added.

Ana Salazar Gonzalez *et al.* (2014) presented a novel method to segment the blood vessels and the Optic Disc proposed a simple method for the blood vessel segmentation and optic disc extraction [42]. The method involves Markov Random field image restoration by removing the blood vessels from the disc region followed by a compensation factor method to extract out the disc.

CHAPTER 3
PROBLEM DEFINITION

Glaucoma is the most leading factor of blindness today. Usually it develops slowly and do not have early stage symptoms and leads to complete vision loss at the later stages. It arises due to the unbalancing or rather the elevation of the eye pressure. The pressure damages the Optic Nerve, shown in Figure 3.1. This eye pressure, called the Inter-Ocular Pressure (IOP), is maintained by the clear fluid in the eye i.e. aqueous humor. An equal amount of this fluid flows in and out of the eye for normal cases. But in abnormal cases, this fluid flow is not proper. Due to this pressure is built [43]. The vision once lost cannot be restored back which makes its early detection even more cognizant.

The disease alters various features of the Fundus image of the eye. A Fundus image of an eye is an optical image which photographs the interior surface of the eye including the retina and has Optic Disc and Optic Cup as its contrasting features. The size and orientation of this Disc and Cup is altered by Glaucoma.

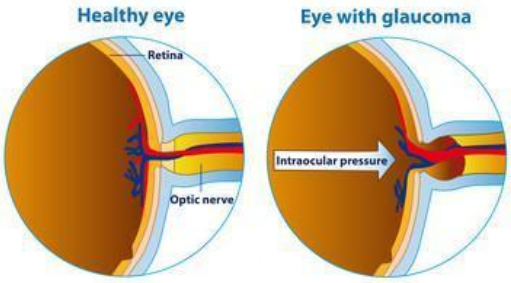

Figure 3.1: Optic Nerve Damage due to elevated pressure [44]

The aim of this dissertation is to evaluate these features, Optic Disc and Optic Cup, of the Fundus images to screen them whether they are suspicious for Glaucoma or not.

CHAPTER 4
PROPOSED SOLUTION

In this dissertation, to screen a Fundus image a total of 50 image samples have been acquired from a local physician. These images are then worked upon to extract the Optic Disc and Optic Cup, and further their diameters using computer aided techniques.

The algorithm for the extraction of Optic Disc and Cup is developed in MATLAB version 8.1.0.604 (R2013a) using the Image Processing Toolbar.

The diameters so obtained are then mathematically divided to obtain a ratio, the Cup-to-Disc Ratio,

Cup-to-Disk Ratio = (Cup diameter) / (Disk diameter)

This ratio is then used for classifying the image samples into normal or suspicious for Glaucoma cases. The classification is done on threshold basis. If the ratio ranges from 0.3 to 0.5, it is considered as normal. But in case this ratio exceeds 0.5, the image sample is considered at risk for Glaucoma.

A Confusion matrix has been plotted to visualize the proposed algorithm‟s performance.

After obtaining the CDR a t-test has been conducted on two groups, namely Normal and suspicious for Glaucomatous. The t-test has been applied to determine whether these two groups are significantly different from each other or not.

CHAPTER 5
PROPOSED METHODOLOGY

5.1 Basic Methodology

For the screening of Glaucoma, the most important feature that is considered is the Cup-to-disc Ratio (CDR). It signals whether the subject is suspicious or not. For the calculation and evaluation of the CDR value, firstly the Optic disc and the Cup are required. The normal CDR values range from 0.3 to 0.5 and values greater than 0.5 are considered suspicious. The basic block diagram of the proposed methodology is shown in Figure 5.1. The methodology proceeds by the conversion of the true color RGB image into Red and Green planes which are then converted to binary images. These images are then operated on with Morphological operations to detect the Optic disk and the Cup.

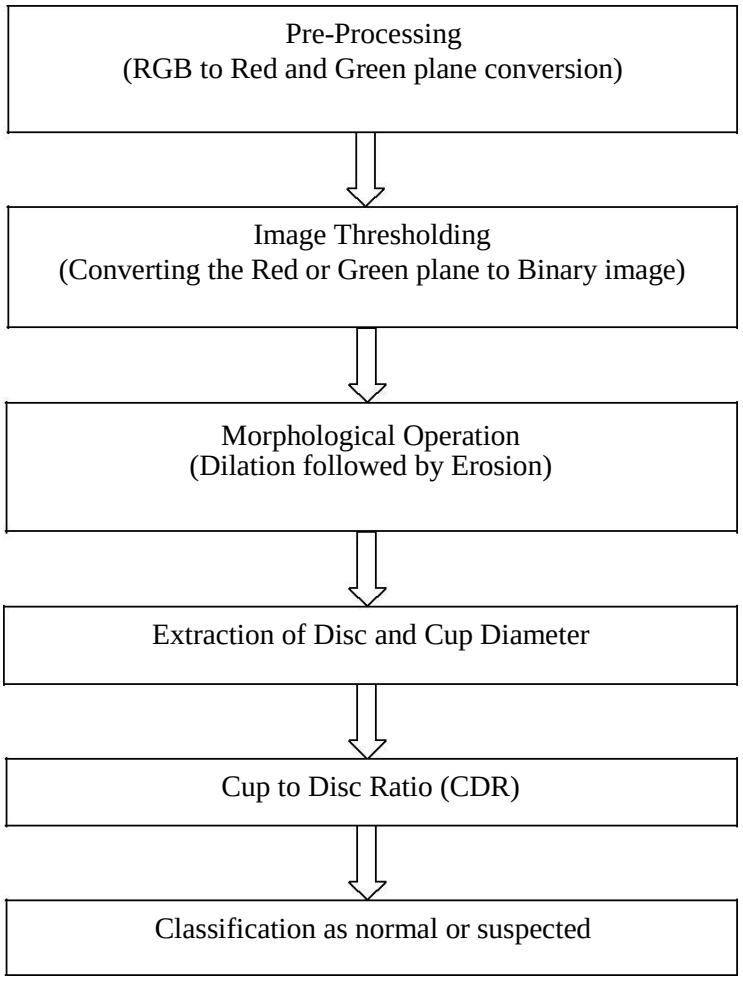

Figure 5.1: Basic Block diagram of the proposed methodology

5.2 Image Preprocessing

The Fundus image is acquired firstly using an Ophthalmoscope or a Fundus camera which is in the RGB format. This RGB image is then analyzed for its contrast levels and after the analysis of a number of retinal images it was concluded that the optic disc has a better contrast in the Red plane and the optic Cup has a better contrast in the Green plane.

Image preprocessing involves the extraction of the Red plane (in case of the optic disc) and the Green plane (in case of optic cup) from the original color retinal fundus image for the extraction of the Disc and the Cup as shown in Figure 5.2.

(a) (b) (c)

Figure 5.2: (a) Original Fundus Image, (b) Red Plane, (c) Green Plane

5.3 Extraction of Optic Disc and Optic Cup

The evaluation of CDR involves the extraction of the Disc and the Cup, to detect the same the Red and Green plane extracted out are then converted into the binary image by thresholding with a specific level or value of threshold for Disc as well as the Cup.

5.3.1 Extraction of Optic Disk

The methodology followed for the extraction of the Disk is given in the Figure 5.3. The image obtained in the pre-processing step is operated upon according to the steps depicted in the flow diagram. The Optic disc is extracted out using thresholding and morphologically operating the pre processed image.

Step 1: Pre-processed Image

The original RGB image is pre processed by converting it into its Red plane as the optic disc has the best contrast in the Red plane. This pre processed image is then applied with further processing steps.

Step 2: Image Thresholding

The Red plane image obtained is then binarized by thresholding it using a fixed level of threshold. The RGB image is first converted into a grayscale image and then converted to the required binary image. The threshold level is kept same for all the images. Thresholding is an important tool that eliminates the parts of an image that are not required. This binary conversion of the Red plane image brings out the details of the image that are hidden and cannot be recognized in the color image. Figure 5.3 shows the output images obtained after applying different steps of the methodology.

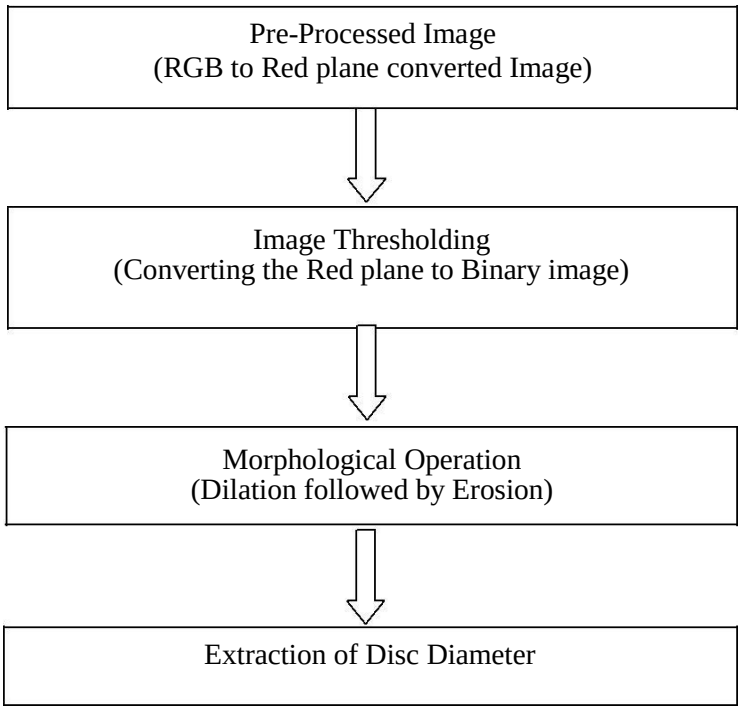

Figure 5.3: Flow diagram for extraction of Optic Disc

Step 3: Morphological Operations

In the extraction of the Optic Disc, the Red plane is first converted to the binary image as mentioned earlier. The binary image so obtained has gaps and uneven boundaries in it. As a remedy for these

gaps and unsymmetrical boundaries, morphological operations are applied to this binary image. The binary image so obtained is applied with the „CLOSE" operation by using the structuring element „DISK". This operation basically involves dilation followed by erosion.

Dilation is one of the core morphological operations that usually use a structuring element for scrutinizing and expanding the shapes in the input image, where a structuring element (SE) is an element or a mask used to probe a given image to check as in on how this shape fits or misses the similar shapes in the image. The mathematical formula for dilation is given in eqn 5.1 and 5.2.

$$A \oplus B = \{z|(\hat{B})_z \cap A \neq \Phi\} \quad \ldots \text{(eqn 5.1)}$$

where *A* is the input image and *B* being the structuring element DISK.

Erosion on the other hand erodes away the boundaries of foreground region i.e. removes structures of certain shape and leads to shrinking of the objects. Erosion can be mathematically expressed as:

$$A \Theta B = \{z|(B)_z \subseteq A\} \quad \ldots \text{(eqn 5.2)}$$

A is again the input image and *B* the structuring element DISK.

The basic concept of these morphological operations can be understood by the Figure 5.4.

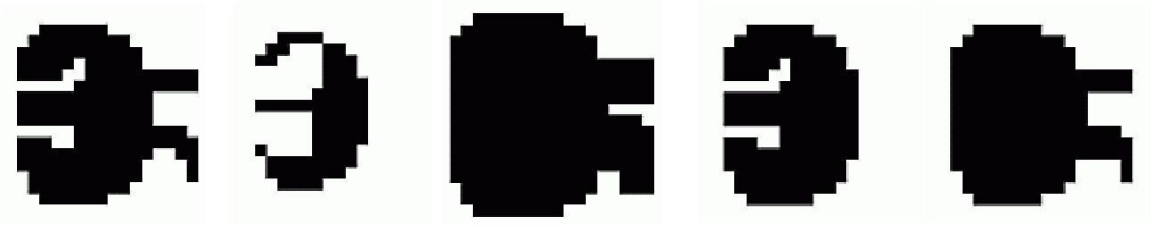

(a) (b) (c) (d) (e)

Figure 5.4: (a) Original Image, (b) Erosion, (c) Dilation, (d) Opening, (e) Closing

The CLOSE operation, as mentioned earlier, is dilation followed by erosion. Due to dilation the diameter of the required cup increases first, but as it is followed by erosion it compensates for the increased dimension (as the structuring element used is same and of same dimension as well). This closing operation fills in all the gaps in the binary image that are held in the Optic Disc and also

smoothes the contour of the extracted disc. Also sometimes the binary image obtained, along with the Disc, contains unwanted areas. To remove these small unwanted parts „Area Opening" is done which provides us with a final image that only contains the Optic Disc and no unwanted areas. Since the optic disk detected is in the form of an ellipse, so the major axis of this ellipse denotes the diameter of the Disc (taken vertically).

Step 4: Disc Diameter

The disc diameter is calculated from the morphologically operated image as the major axis of the ellipse so obtained. The diameter is extracted as the major axis because the measurements are taken vertically according to the gold standards.

5.3.2 Extraction of Optic Cup

The extraction of the cup involves the same methodology of plane conversion of the original retinal fundus image and then thresholding and finally the cup diameter.

Step 1: Pre-processed Image

The original RGB image is pre processed by converting it into its Green plane as the optic Cup, unlike Disc, has best contrast in the Green plane.

Step 2: Image Thresholding

The Green plane image obtained is then converted into its binary form by thresholding it using a fixed level of threshold (a threshold value different from the one used for the Disc). This RGB to binary conversion involves the conversion into a grayscale image and then to the required binary image. The threshold level is fixed for all the samples. The threshold value used in case of the Cup is kept lower than the one used for the Disc.

Step 3: Morphological Operations

This binary image so obtained again contains the optic cup but with irregular gaps. These gaps are then filled by using the morphological operation „CLOSING" using the „DISK" structuring element, the same way as in case of Disc detection, but with a different radius from the one used for Disc

detection. The morphology used in case of the Cup is similar to the one used in case of the Disc. The flow diagram for Cup diameter extraction can be understood by Figure 5.5.

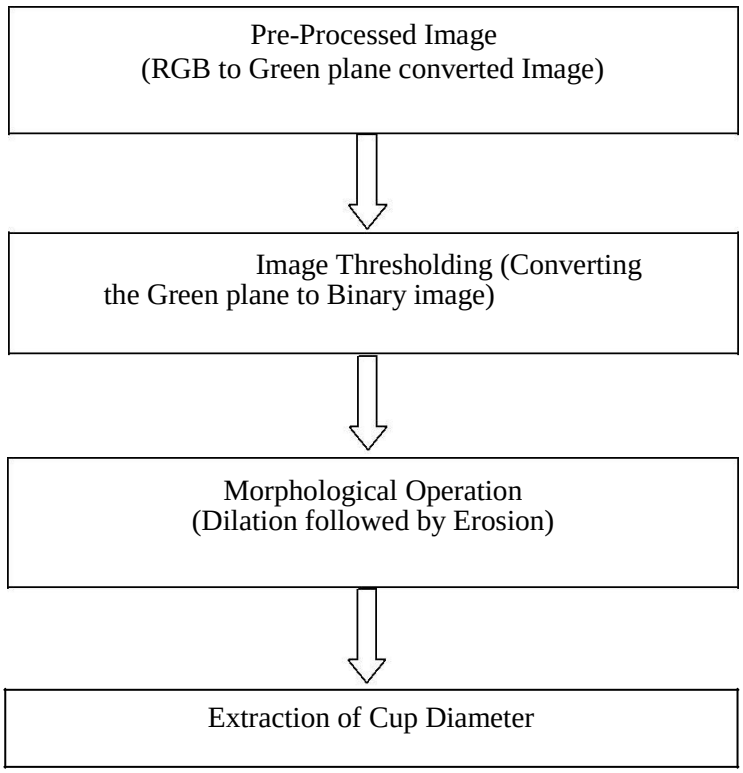

Figure 5.5: Flow diagram for extraction of Optic Cup

Step 4: Cup Diameter

The Cup diameter is also calculated from the morphologically operated image as the major axis of the ellipse so obtained. The diameter is extracted as the major axis because the measurements are taken vertically according to the gold standards.

5.4 Cup-To-Disc Ratio Calculation

The Cup-to-Disc ratio is denoted as the ratio of the diameter of the cup to that of the disc. It is calculated by mathematically dividing the value of Cup diameter by the Disk diameter (taken vertically),

Cup-to-Disk Ratio = (Cup diameter) / (Disk diameter)

The values obtained are the CDR values which are further used for the classification of the images or subjects as normal or suspicious for Glaucoma. The images with CDR values ranging from 0.3 to 0.5 are classified as the normal ones and those with values greater than 0.5 are screened for Glaucoma or are considered at risk for Glaucoma.

CHAPTER 6
RESULTS AND DISCUSSIONS

6.1 Results Of Pre-Processing

This section explains the results of the algorithm used. The pre-processing as explained earlier involves the conversion of the color retinal fundus image into their required Red and Green planes from Optic Disc and Optic Cup shown in Figure 6.1.

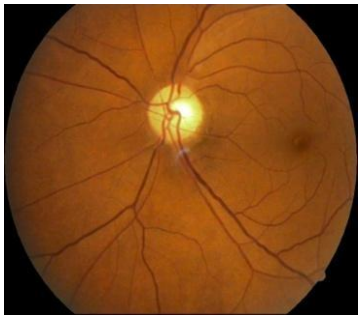

(a)

(b)

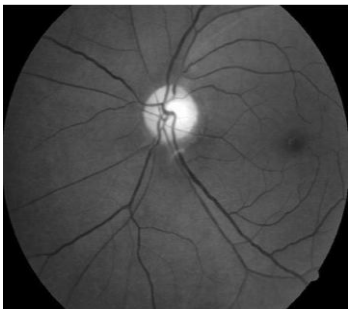

(c)

Figure 6.1: (a) Original Fundus Image, (b) Red Plane, (c) Green Plane

The algorithm has been applied to a database acquired from a local physician. After the analysis of a number of samples, the red and the green plane were best suitable for extracting disc and the cup respectively from the contrast point of view. The database consisted of 50 images, with 21 Glaucomatous and 29 normal images. The red and green planes show the best versions of Optic Disc and the Optic Cup. The binary conversions of these RGB planes bring out the required regions much easily and efficiently.

6.2 Results Of Extraction Of Optic Disc

The results of the methodology followed for extracting the Optic Disc are explained in this section. The Optic Disc is the most contrasting feature of a retinal fundus image. The methodology applied is compared with other proposed methods and it is observed that it is the simplest method to extract out the Optic Disc. The methodology involves the basic morphological processes unlike other complex methods that have been followed so far and provides with efficient results.

Step 1: Pre-processed Image: As mentioned earlier, for the extraction of Optic Disc the red plane is first extracted out shown below in Figure 6.2.

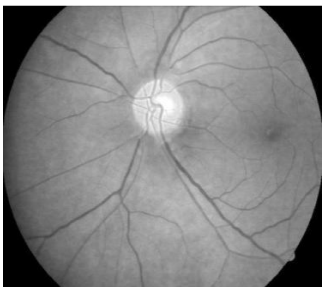

Figure 6.2: Pre-Processed Image (Red plane)

*Step 2***:** The results of the image thresholding, i.e. red plane to binary conversion as shown in Figure 6.3.

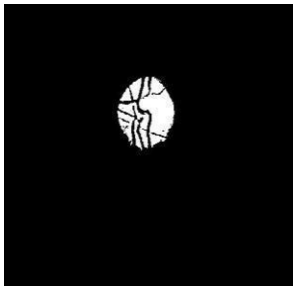

Figure 6.3: Binary Optic disc after thresholding

*Step 3***:** The binary image so obtained after thresholding comes with irregular gaps and uneven boundaries. These gaps as explained earlier are eliminated by operating the image with morphological operations Dilation and Erosion using a specific Structuring element. These two operations when performed in this order, i.e. dilation followed by erosion, is also known as Closing operation. The resultant image after performing theses operations is shown in Figure 6.4.

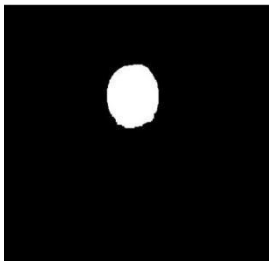

Figure 6.4: Morphologically Operated Disc

6.3 Results Of Extraction Of Optic Cup

The steps for the extraction of Optic Cup from the fundus image are explained in this section. The changes in the area and size of the Optic Cup in a fundus image signify the sample image‟s condition whether normal or suspicious.

Step 1: Pre-processed Image: For the extraction of Optic Cup the green plane extracted out is shown in Figure 6.5 below. This pre processed image is further operated with using thresholding and morphology.

Figure 6.5: Pre-Processed Image (Green plane)

Step 2: The image thresholding, i.e. green plane to binary conversion is shown in the Figure 6.6.

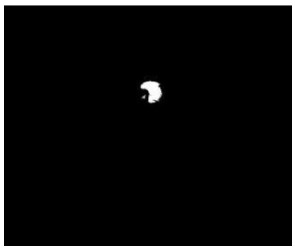

Figure 6.6: Binary Optic Cup after thresholding

Step 3: Just as the binary operated disc came with some irregularities the optic cup also came with a few gaps and incomplete boundaries. To detect the complete shape of the cup the binary operated disc has to be operated with morphological operations to cover for these incomplete boundaries and irregular shape. The final cup detected after morphology has been shown in the Figure 6.7.

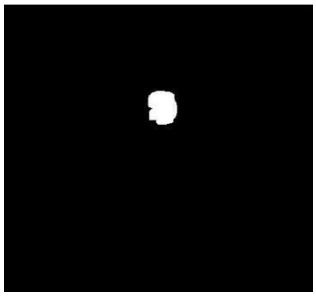

Figure 6.7: Morphologically Operated Disc

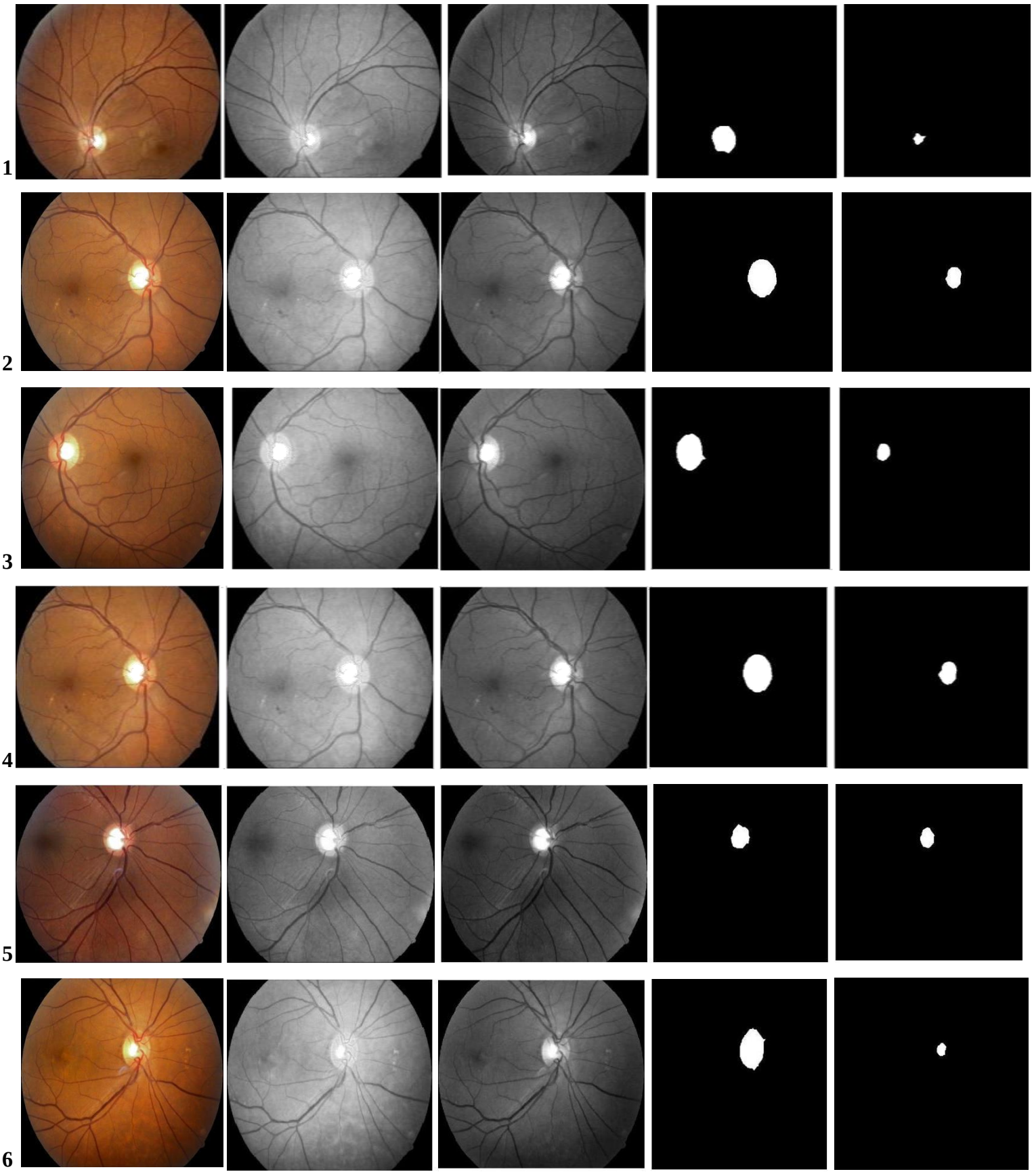
1
2
3
4
5
6

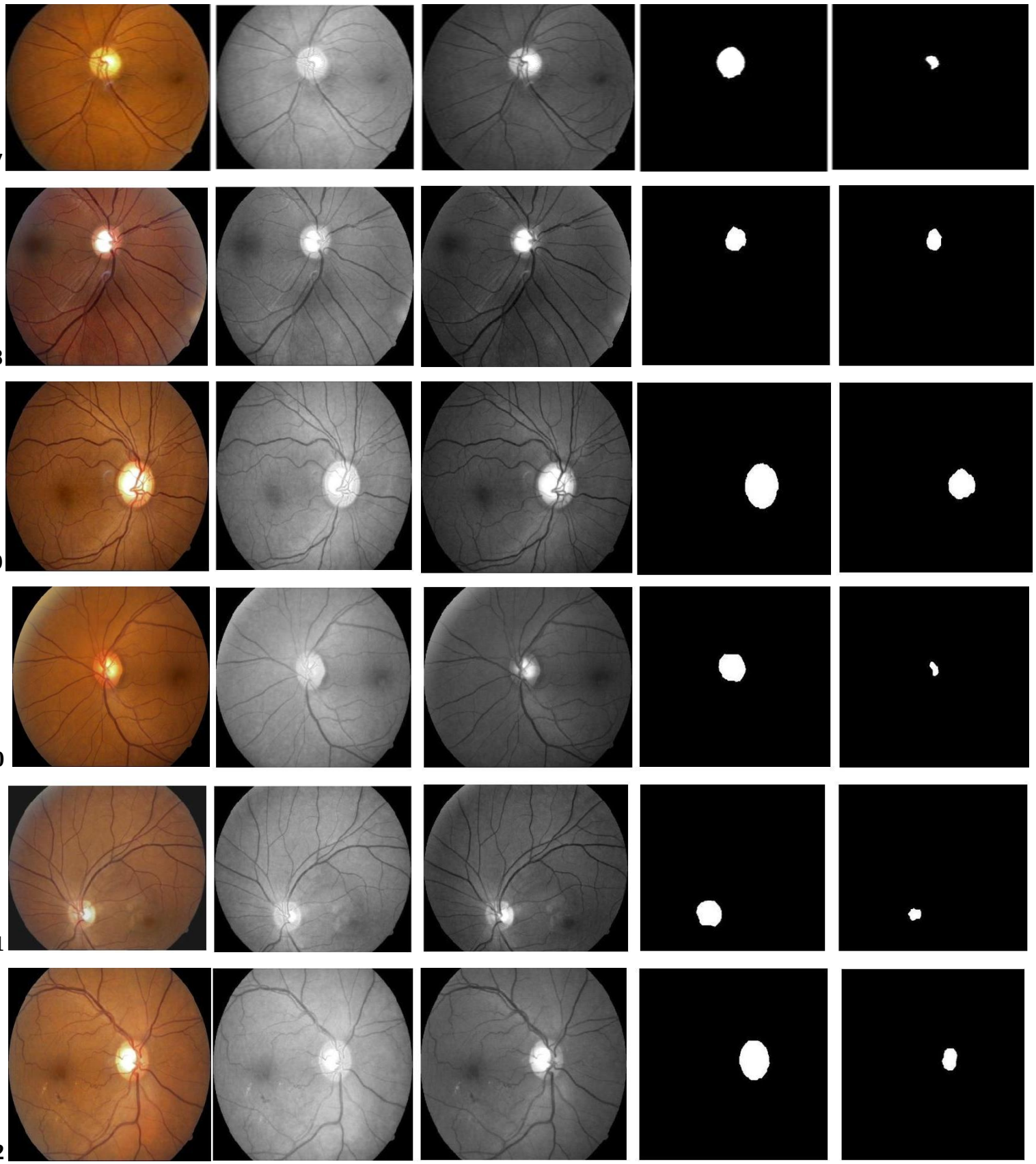
7
8
9
10
11
12

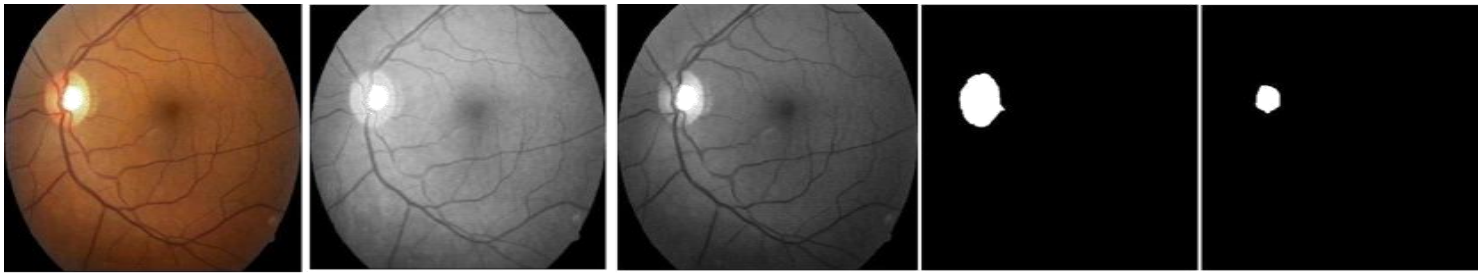

14

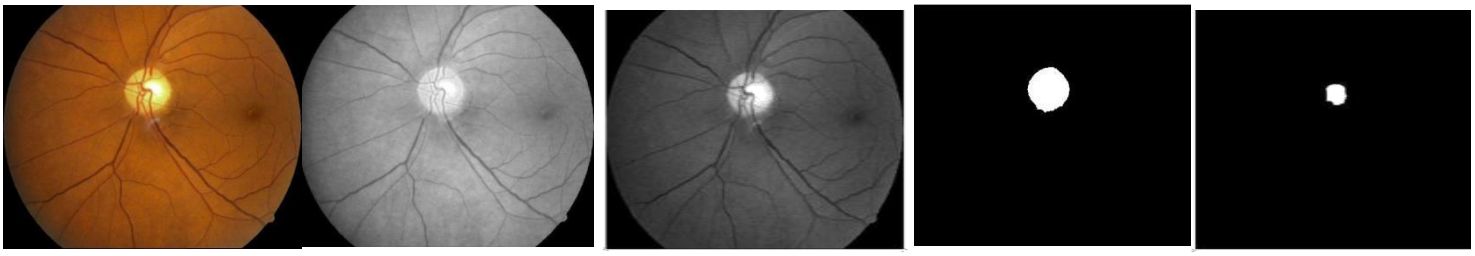

16

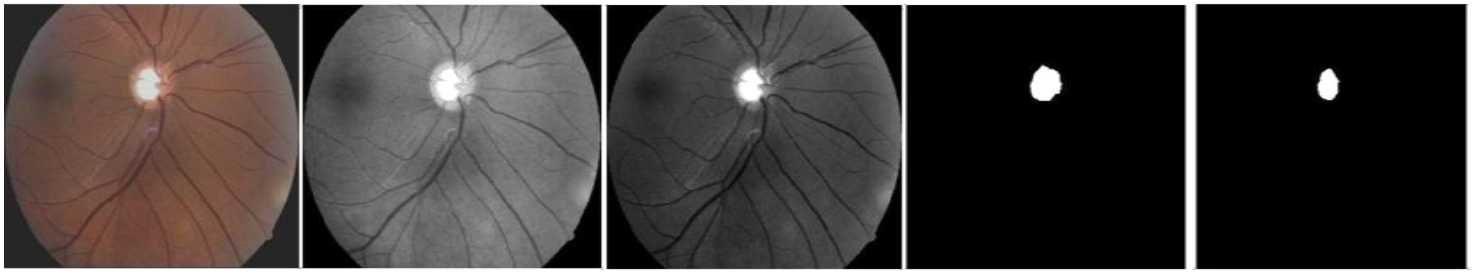

18

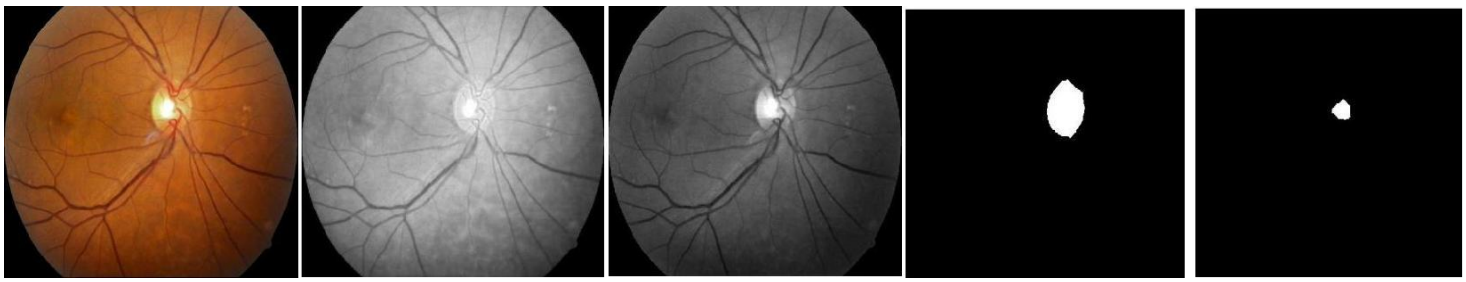

19

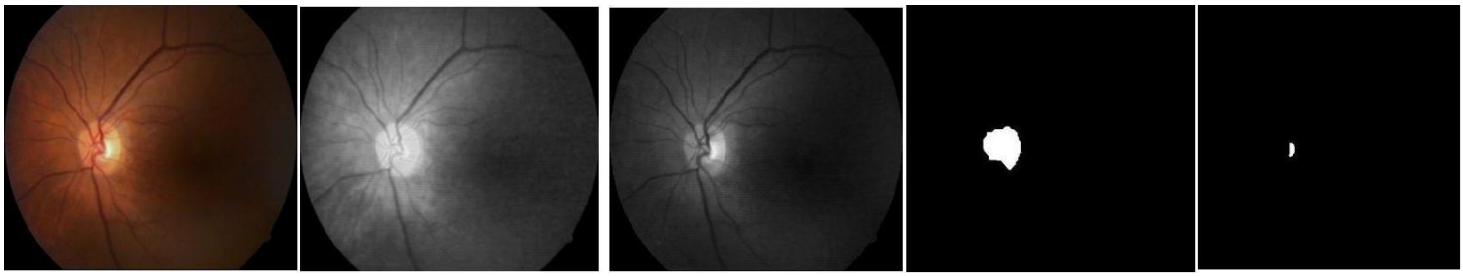

22

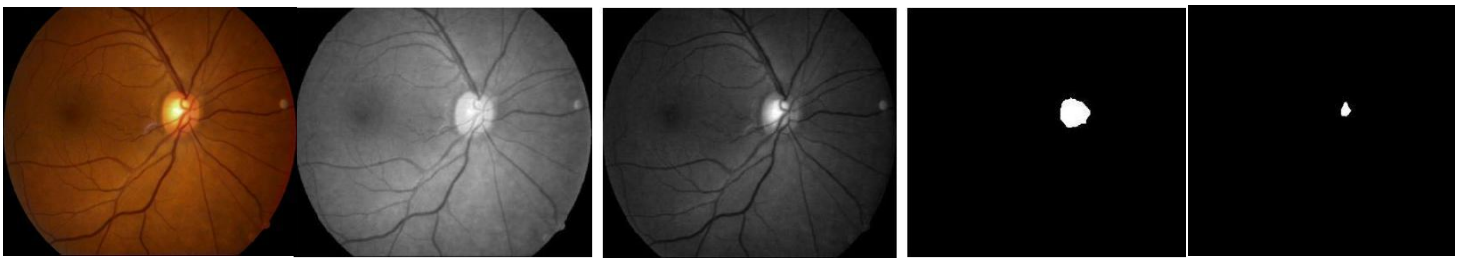

24

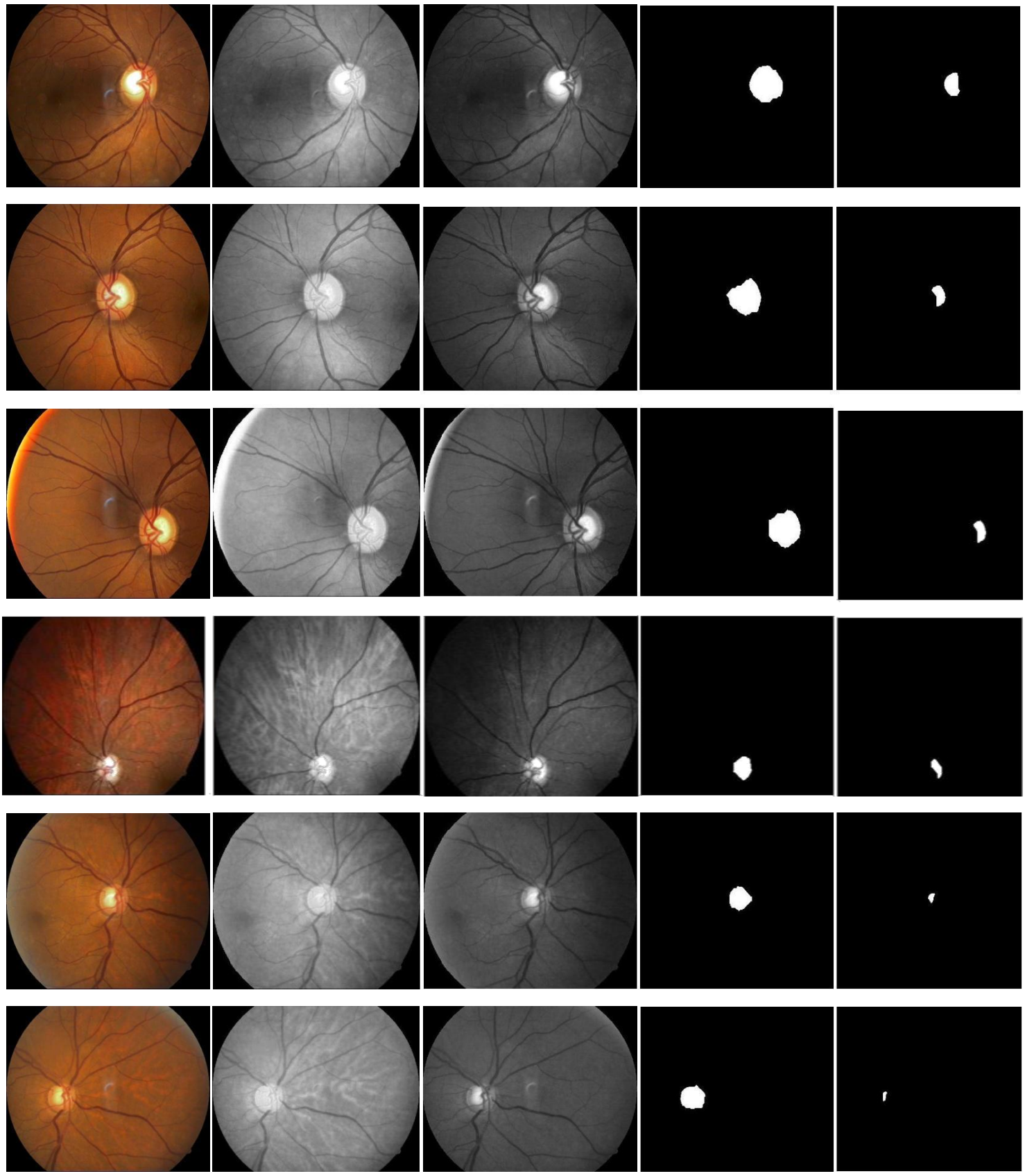
26
27
28
29
30
31

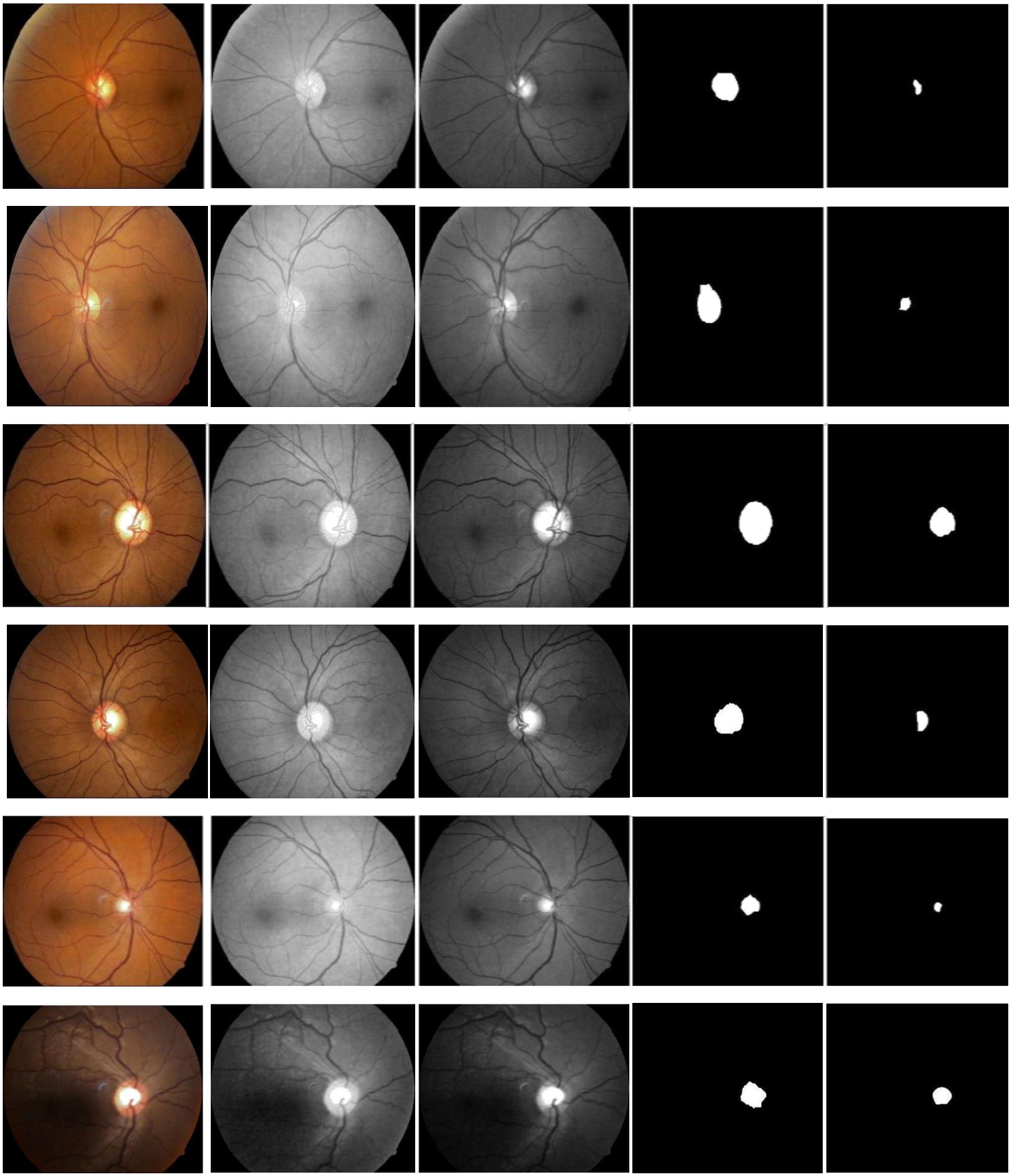
33
34
35
36
37
38

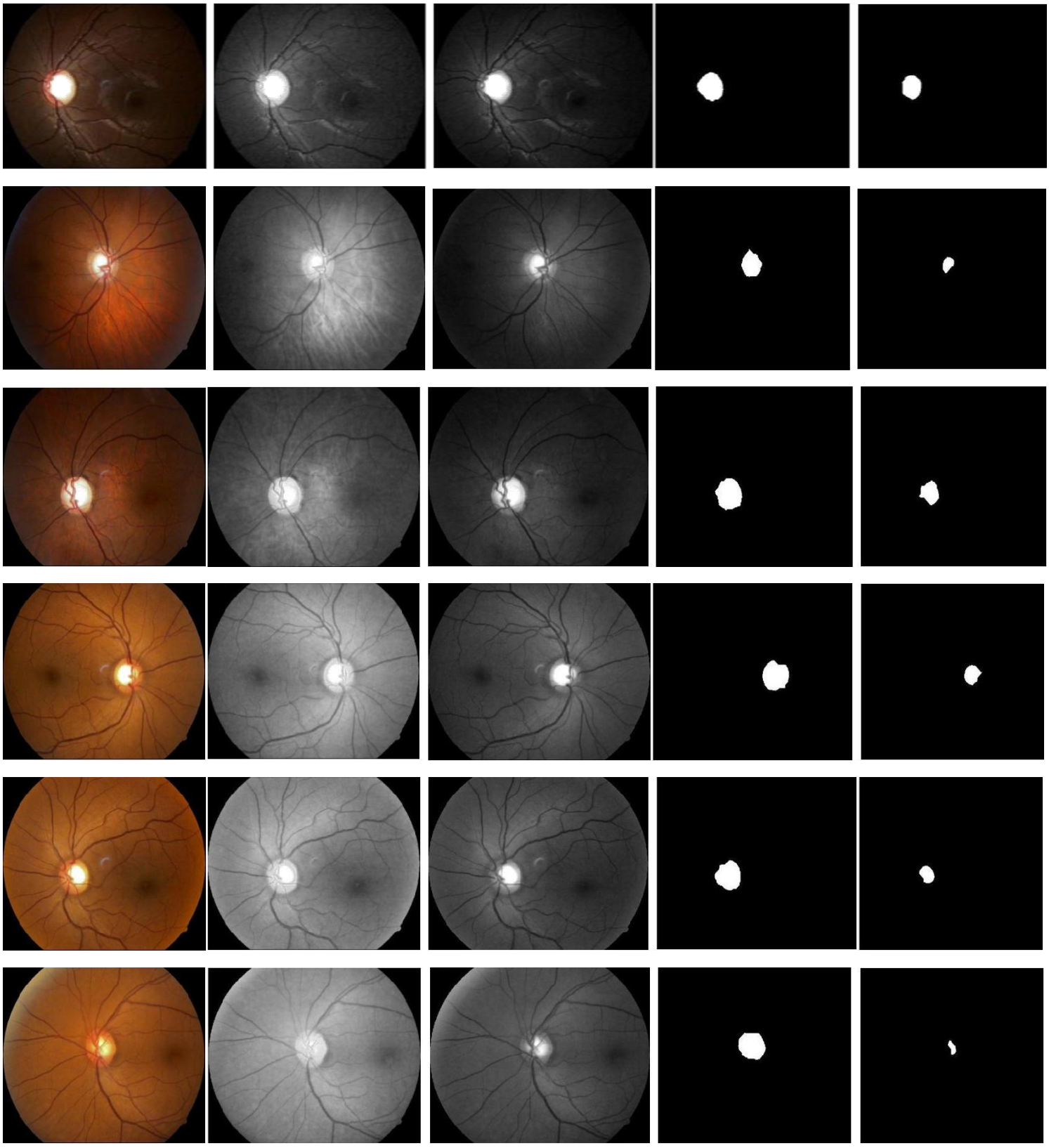
39
41
42
44
45
46

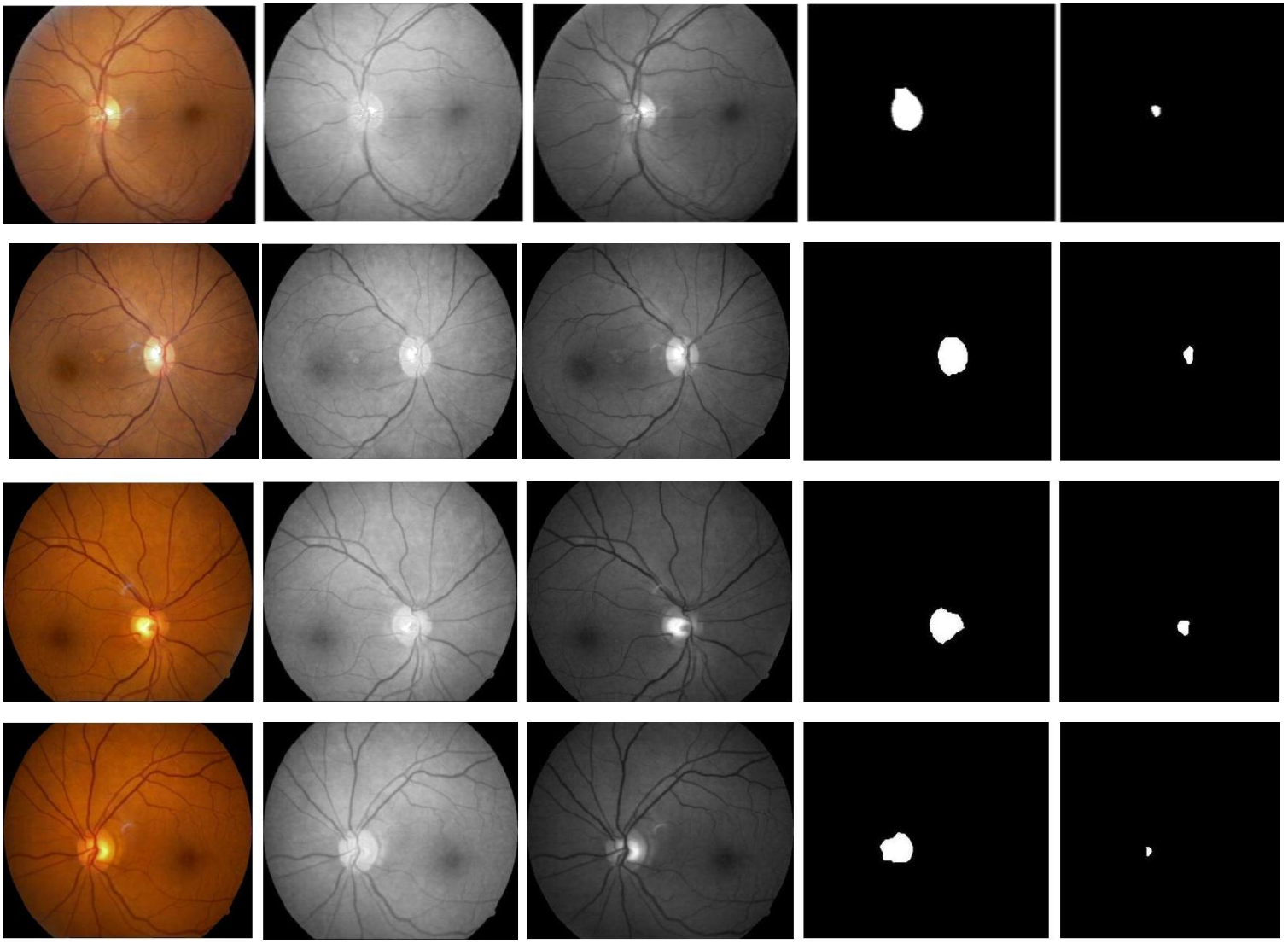

re 6.8: (a) First column represents Original color retinal Fundus images (b) Second and Third column represents the results of Pre-processing (Red plane and green plane images) (c) Fourth column represents the extracted Optic Disc (d) Fifth column represents the extracted Optic Cup

6.4 Results Of Cup-To-Disc Ratio Calculations

The methodology is applied on a total of 50 images. The results of the methodology are compared with the gold standard values provided by the physician values. Table 6.1-6.2 and Figure 6.9 (a)-(e) shows the comparison of the measured and the true CDR values of the Cup as well as the disc. The values of the Disc and cup diameter are measured using a fixed threshold.

Table 6.1: Comparison of Measured and True CDR Value (Sample 1-25)

Sample no.	Disk		Cup		CDR(Measured) = Cup(measured)/ Disk(measured)	CDR(True) = Cup(true)/ Disk(true)	Measured	True
	Measured	True	Measured	True				
1	98	96	40	41	0.39	0.40	Normal	Normal
2	120	123	68	68	0.56	0.55	Glaucomatous	Glaucomatous
3	114	120	55	52	0.50	0.43	Normal	Normal
4	121	119	73	64	0.60	0.54	Glaucomatous	Glaucomatous
5	80	107	66	67	0.8	0.62	Glaucomatous	Glaucomatous
6	120	112	40	45	0.34	0.40	Normal	Normal
7	106	104	50	38	0.47	0.36	Normal	Normal
8	79	108	69	68	0.80	0.63	Glaucomatous	Glaucomatous
9	134	139	98	80	0.73	0.60	Glaucomatous	Glaucomatous
10	103	122	50	55	0.48	0.45	Normal	Normal
11	978	95	39	46	0.40	0.48	Normal	Normal
12	120	121	69	68	0.57	0.56	Glaucomatous	Glaucomatous
13	100	104	-	57	-	0.54	-	Glaucomatous
14	114	120	54	58	0.47	0.48	Normal	Normal
15	80	108	-	59	-	0.54	-	Glaucomatous
16	106	102	50	41	0.47	0.40	Normal	Normal
17	82	107	-	43	-	0.40	-	Normal
18	80	106	66	70	0.8	0.66	Glaucomatous	Glaucomatous
19	130	109	40	44	0.30	0.40	Normal	Normal
20	92	97	-	26	-	0.30	-	Normal
21	101	129	-	50	-	0.38	-	Normal
22	96	107	26	45	0.30	0.42	Normal	Normal
23	93	117	-	30	-	0.30	-	Normal
24	78	110	25	41	0.32	0.37	Normal	Normal
25	74	109	-	43	-	0.39	-	Normal

Table 6.2: Comparison of Measured and True CDR Value (Sample 26-50)

Sample no.	Disk		Cup		CDR(Measured) = Cup(measured)/ Disk(measured)	CDR(True) = Cup(true)/ Disk(true)	Inference (Measured)	Inference (True)
	Measured	True	Measured	True				
26	122	121	70	57	0.57	0.47	Glaucomatous	Normal
27	122	144	62	58	0.5	0.40	Normal	Normal
28	120	143	52	63	0.50	0.44	Normal	Normal
29	70	112	62	74	0.8	0.66	Glaucomatous	Glaucomatous
30	82	97	25	36	0.30	0.37	Normal	Normal
31	93	92	26	34	0.30	0.36	Normal	Normal
32	106	95	-	27	-	0.28	-	Normal
33	103	114	43	43	0.40	0.37	Normal	Normal
34	114	92	31	31	0.30	0.34	Normal	Normal
35	134	141	97	88	0.70	0.62	Glaucomatous	Glaucomatous
36	112	132	68	76	0.60	0.57	Glaucomatous	Glaucomatous
37	62	92	31	46	0.52	0.51	Glaucomatous	Glaucomatous
38	105	126	73	59	0.60	0.46	Glaucomatous	Normal
39	100	125	82	85	0.80	0.68	Glaucomatous	Glaucomatous
40	108	107	-	63	-	0.58	-	Normal
41	78	117	53	70	0.60	0.59	Glaucomatous	Glaucomatous
42	97	118	74	89	0.70	0.70	Glaucomatous	Glaucomatous
43	84	114	-	65	-	0.57	-	Glaucomatous
44	96	112	63	64	0.60	0.57	Glaucomatous	Glaucomatous
45	94	115	62	61	0.60	0.53	Glaucomatous	Glaucomatous
46	103	112	53	69	0.52	0.61	Glaucomatous	Glaucomatous
47	114	97	46	41	0.40	0.42	Normal	Normal
48	101	107	52	45	0.50	0.42	Normal	Normal
49	96	107	44	51	0.45	0.47	Normal	Normal
50	97	111	38	50	0.39	0.45	Normal	Normal

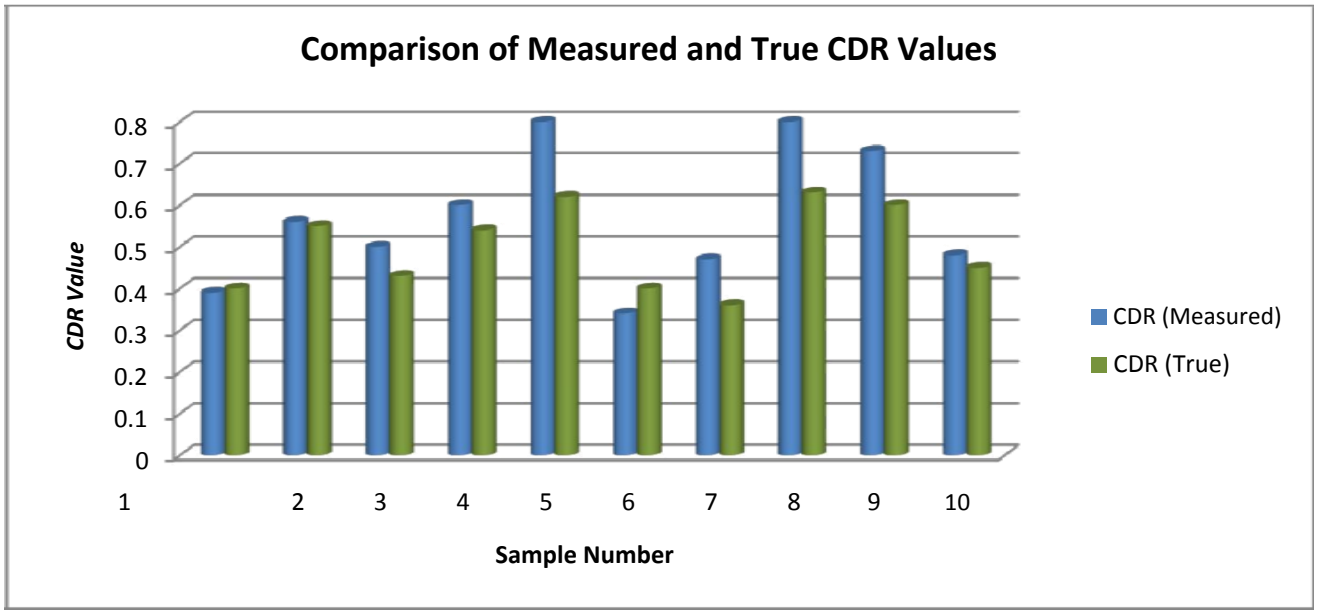

Figure 6.9 (a)**:** Comparison of Measured and True CDR Value (Sample 1-10)

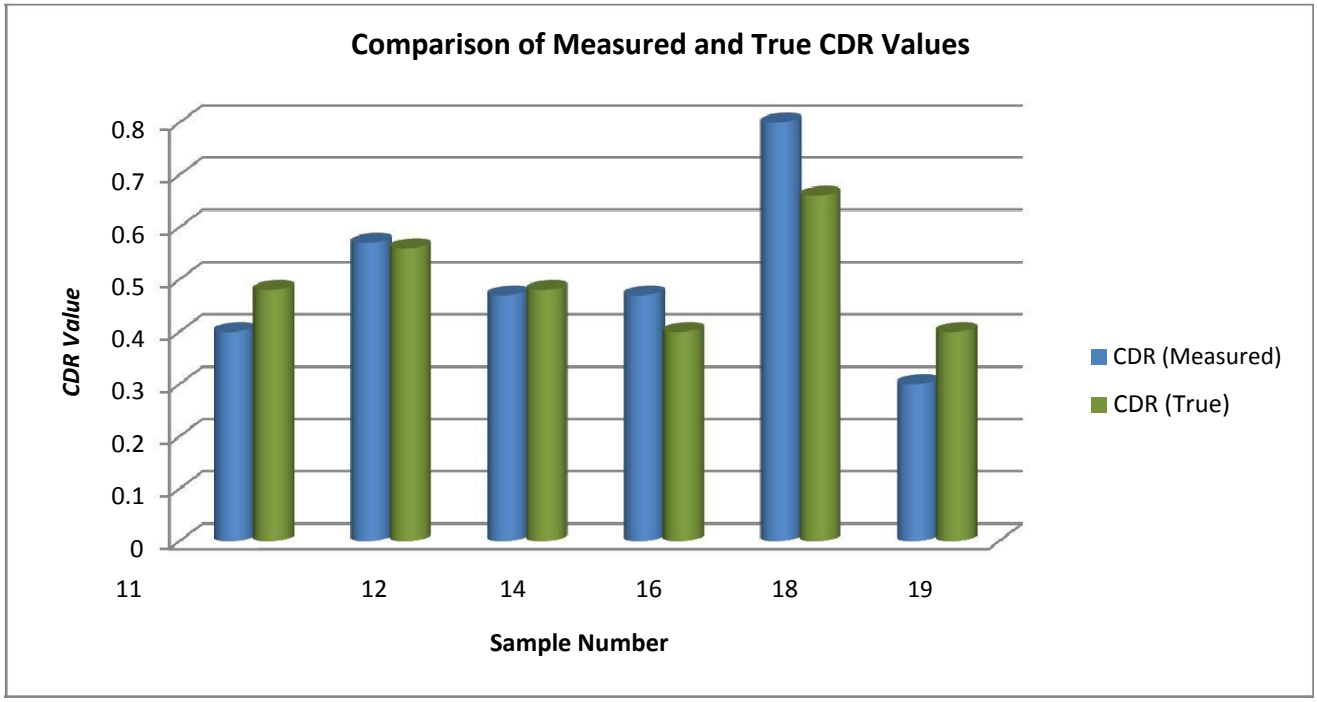

Figure 6.9 (b)**:** Comparison of Measured and True CDR Value (Sample 11-20)

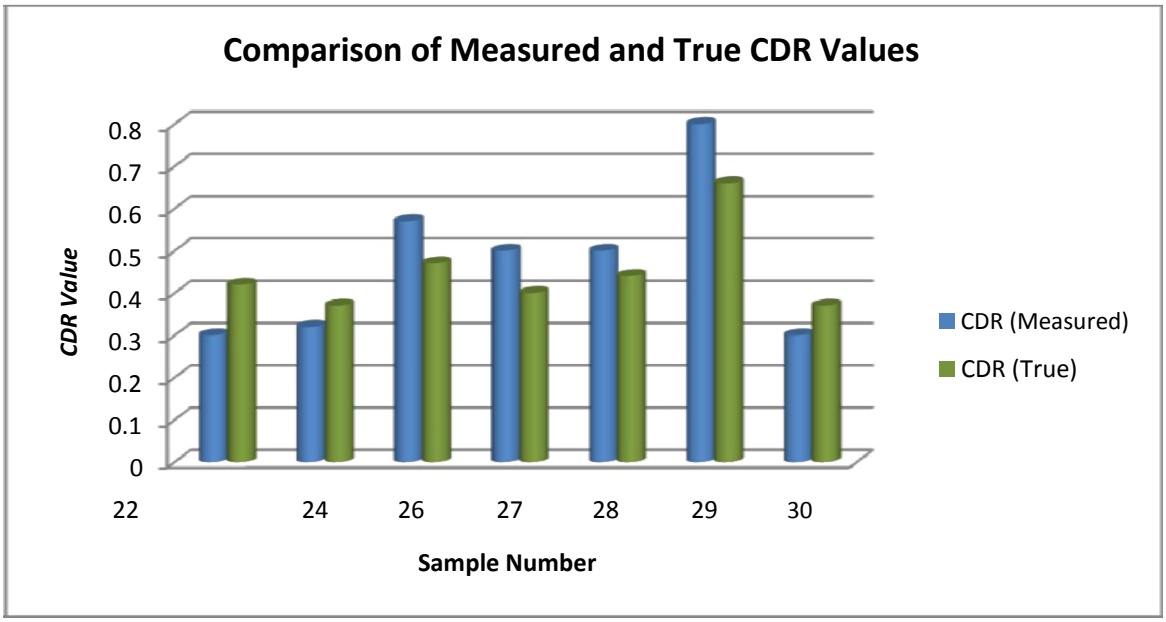

Figure 6.9 (c)**:** Comparison of Measured and True CDR Value (Sample 21-30)

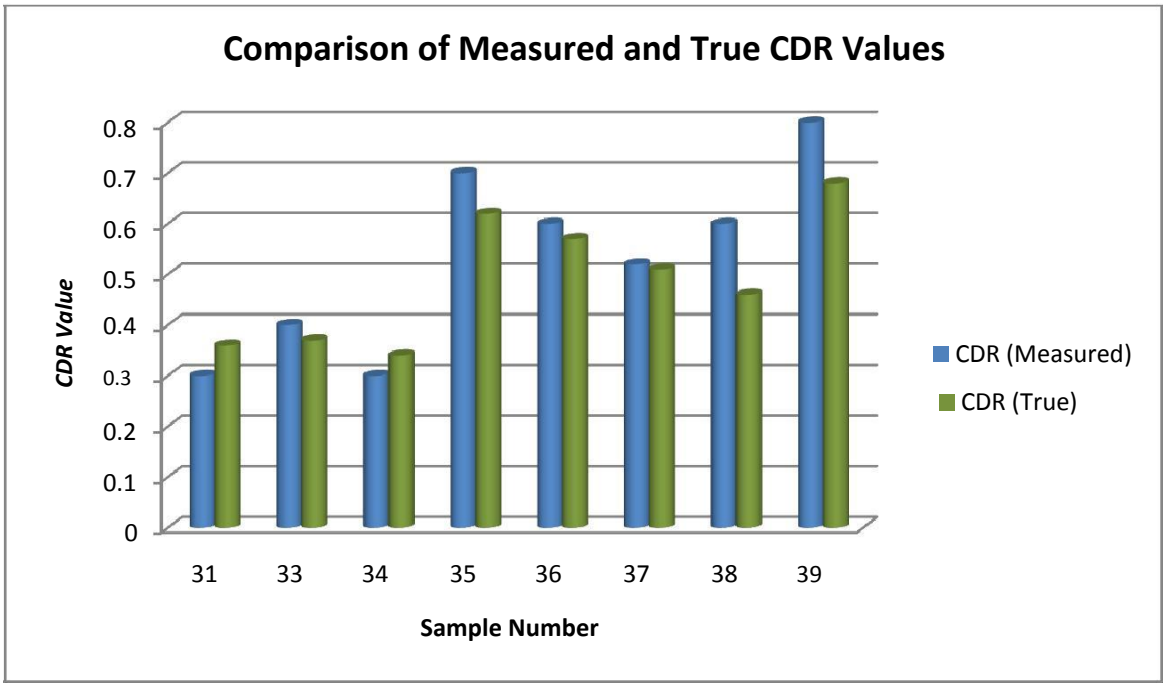

Figure 6.9 (d)**:** Comparison of Measured and True CDR Value (Sample 31-40)

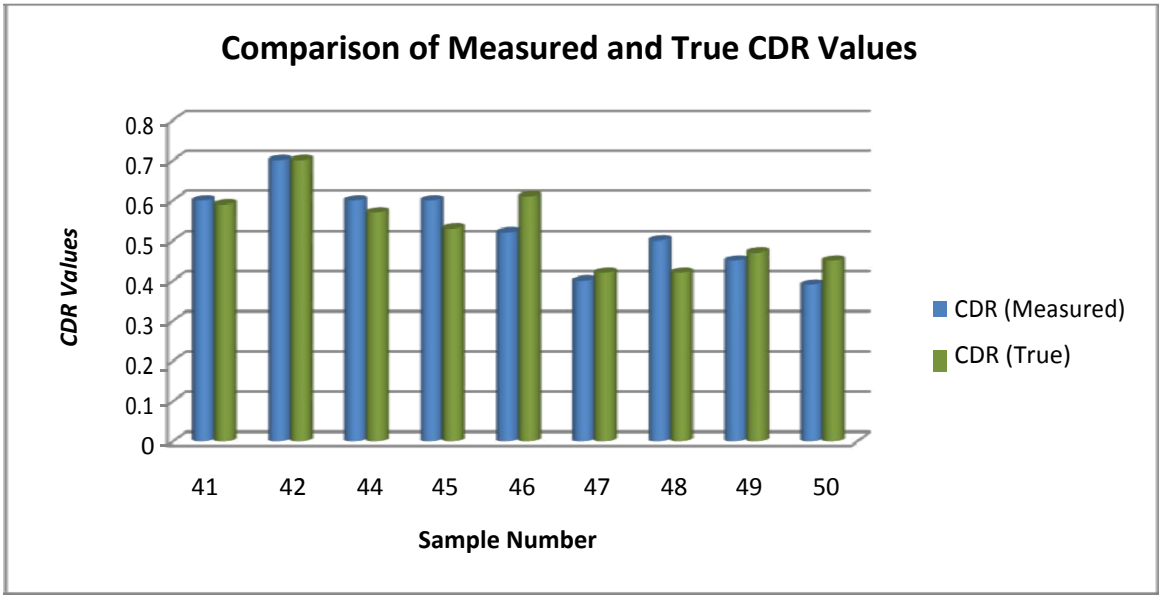

Figure 6.9 (e)**:** Comparison of Measured and True CDR Value (Sample 41-50)

6.5 Evaluating Predictive Parameters

Since the results of the classification of the sample images by the techniques used depends upon the image quality and also on the user experience. To visualize the performance of the algorithm proposed, a confusion matrix is plotted [45]. This matrix consists of predicted class and actual class instances as shown in the Figure 6.10.

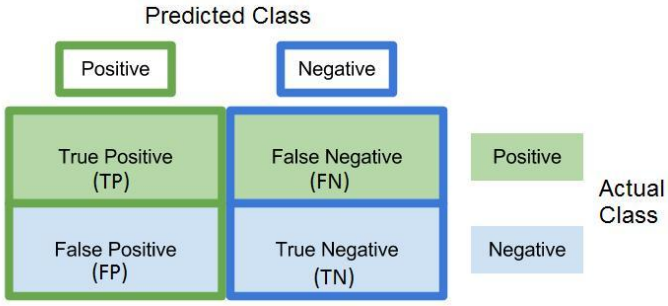

Figure 6.10: Confusion Matrix

TP (true positive) here depicts the number of samples correctly classified as Glaucomatous. TN (true negative) signifies the number of samples correctly classified as normal samples. FN (false negative)

and FP (false positive) signifies the number of samples incorrectly classified as normal and Glaucomatous respectively. The confusion matrix with proposed algorithm instances is shown in Figure 6.11. These instances are used to formulate predictive parameters that are going to analyze the algorithm‟s performance.

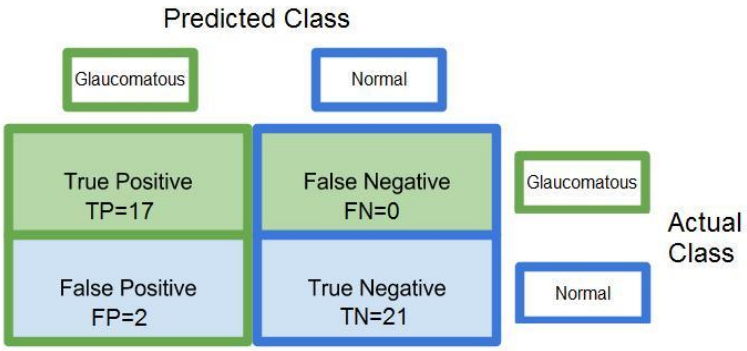

Figure 6.11: Confusion Matrix with Proposed Algorithm Instances

These predictive parameters are Sensitivity, Specificity, Accuracy, Positive Predictive Value (PPV), Negative Predictive Value (NPV), False Positive rate (FPR), False Discovery Rate (FDR), False Negative Rate (FNR) and F1 Score.

Sensitivity, also known as the True Positive rate, measures the positive proportion correctly classified according to the given conditions. It can be calculated as the ratio of true positive to the sum of true positive and false negative.

$$\text{Sensitivity} = TP/ (TP+FN)$$

Specificity, also known as True Negative Rate, measures the negative proportion correctly classified as such. It can be formulated by taking the ration of true negative to the sum of true negative and false positive.

$$\text{Specificity} = TN/ (TN+FP)$$

Accuracy refers to basically the proximity of the measured results to the true values. It can be calculated as,

$$\text{Accuracy} = (TP+TN)/ (TN+TP+FN+FP)$$

Positive Predictive Value, also known as Precision, indicates as in how best the algorithm can detect the samples correctly. It can be stated as the ratio true positives to the sum of true positives and false positives.

$$PPV = TP/ (TP+FP)$$

Negative Predictive Value depicts the negative proportion results in the statistics results.

$$NPV = TN/ (TN+FN)$$

False Positive Rate, during multiple comparisons, refers to the chances of falsely rejecting the theory that there is no relation between any measured groups or phenomenon.

$$FPR = FP/ (FP+TN)$$

False Discovery Rate can be denoted as expected percentage of false predictions in a set of different predictions.

$$FDR = FP/ (FP+TP)$$

False Negative Rate is a value in which a test result falsely indicates no presence, when in reality it is present.

$$FNR = FN/ (FP+TP)$$

F1 score basically measures the algorithm‟s accuracy [45].

$$F1\ score = 2TP/ (2TP+FP+FN)$$

Table 6.3 and Table 6.4 show the predictive parameter values and the Test Outcomes respectively.

Table 6.3: Predictive Parameter Values

True Positive (TP)	**False Positive (FP)**	**True Negative (TN)**	**False Negative (FN)**
17	2	21	0

Table 6.4: Test Outcomes

S. No.	Parameter	Expression	Value
1	Accuracy (%)	(TP+TN)/(P+N)	95
2	Sensitivity (%)	TP/(TP+FN)	100
3	Specificity (%)	TN/(TN+FP)	91
4	Precision or Positive Predictive Value (PPV)	TP/(TP+FP)	0.89
5	Negative Predictive Value (NPV)	TN/(TN+FN)	1
6	False Positive Rate (FPR) (%)	FP/(FP+TN)	86
7	False Discovery Rate (FDR) (%)	FP/(FP+TP)	10
8	False Negative Rate (FNR) (%)	FN/(FN+TP)	0
9	F1 Score	2TP/(2TP+FP+FN)	0.94

6.6 Student's T-Test

A t-test is a hypothesis test which is used to determine if two groups of data significantly differ from each other or not. It can be applied if the test statistics are following a normal distribution. It is basically used for analyzing the statistical significance of mean difference of two samples [46]. The two-sample t-test used compares the means of the first group minus the mean of the second group to a specific threshold.

The t-test has been conducted on two groups namely, normal and glaucomatous, in MS excel. The mean and standard deviation of the CDR value from the table are shown in Table 6.5. It can be seen from the table that the CDR value is higher for Glaucomatous cases as compared to the normal ones. As a result of this test the *P*-value for both the groups came out to be 6.06085E-09 i.e. <0.0001, which indicated that the two groups are extremely statistically significant with 95% confidence interval from -0.3077 to -0.1923.

Table 6.5: Mean and Standard Deviation values of CDR with P value

Normal Mean	Normal Standard Deviation	Glaucomatous Mean	Glaucomatous Standard Deviation	P- Value
0.40	0.08	0.65	0.10	<0.0001

6.7 Compensated Cup-to-Disc Ratio (CDR) for Minimized Mean Square Error (MSE)

The CDR values observed from the proposed methodology were on a slightly higher side. To compensate for these higher values, compensation factors of 0.98 and 0.97 are used and their results are then compared, shown in Table 6.6 and Table 6.7.

Table 6.6: Comparison of Compensated CDR values with $\alpha = 0.98$

S. no.	CDR (True)	CDR (Measured)	CDR (Compensated) = CDR (Measured)*0.98	Uncompensated Error= CDR (True – Measured)	Compensated Error= CDR (True-Compensated)	Uncompensated Error Square	Compensated Error Square
1	0.427	0.408	0.4	0.019	0.027	0.000361	0.000729
2	0.553	0.567	0.555	-0.014	-0.002	0.000196	4E-06
3	0.433	0.482	0.473	-0.049	-0.04	0.002401	0.0016
4	0.538	0.603	0.591	-0.065	-0.053	0.004225	0.002809
5	0.626	0.825	0.809	-0.199	-0.183	0.039601	0.033489
6	0.402	0.333	0.327	0.069	0.075	0.004761	0.005625
7	0.365	0.472	0.462	-0.107	-0.097	0.011449	0.009409
8	0.63	0.873	0.856	-0.243	-0.226	0.059049	0.051076
9	0.576	0.731	0.717	-0.155	-0.141	0.024025	0.019881
10	0.451	0.485	0.476	-0.034	-0.025	0.001156	0.000625
11	0.484	0.398	0.39	0.086	0.094	0.007396	0.008836
12	0.562	0.575	0.564	-0.013	-0.002	0.000169	4E-06
14	0.483	0.474	0.464	0.009	0.019	8.1E-05	0.000361
16	0.402	0.472	0.462	-0.07	-0.06	0.0049	0.0036
18	0.66	0.825	0.809	-0.165	-0.149	0.027225	0.022201
19	0.404	0.308	0.302	0.096	0.102	0.009216	0.010404
22	0.421	0.271	0.265	0.15	0.156	0.0225	0.024336
24	0.373	0.321	0.314	0.052	0.059	0.002704	0.003481
26	0.471	0.574	0.562	-0.103	-0.091	0.010609	0.008281
27	0.403	0.508	0.498	-0.105	-0.095	0.011025	0.009025
28	0.441	0.433	0.425	0.008	0.016	6.4E-05	0.000256
29	0.661	0.886	0.868	-0.225	-0.207	0.050625	0.042849
30	0.371	0.305	0.299	0.066	0.072	0.004356	0.005184

S. no.	CDR (True)	CDR (Measured)	CDR (Compensated) = CDR (Measured)*0.98	Uncompensated Error= CDR (True – Measured)	Compensated Error= CDR (True-Compensated)	Uncompensated Error Square	Compensated Error Square
31	0.37	0.28	0.274	0.09	0.096	0.0081	0.009216
33	0.377	0.417	0.409	-0.04	-0.032	0.0016	0.001024
34	0.337	0.272	0.266	0.065	0.071	0.004225	0.005041
35	0.624	0.724	0.709	-0.1	-0.085	0.01	0.007225
36	0.576	0.607	0.595	-0.031	-0.019	0.000961	0.000361
37	0.5	0.5	0.49	0	0.01	0	0.0001
38	0.468	0.695	0.681	-0.227	-0.213	0.051529	0.045369
39	0.68	0.82	0.804	-0.14	-0.124	0.0196	0.015376
41	0.598	0.679	0.666	-0.081	-0.068	0.006561	0.004624
42	0.754	0.763	0.748	-0.009	0.006	8.1E-05	3.6E-05
44	0.571	0.656	0.643	-0.085	-0.072	0.007225	0.005184
45	0.53	0.66	0.646	-0.13	-0.116	0.0169	0.013456
46	0.616	0.515	0.504	0.101	0.112	0.010201	0.012544
47	0.423	0.404	0.395	0.019	0.028	0.000361	0.000784
48	0.421	0.515	0.505	-0.094	-0.084	0.008836	0.007056
49	0.477	0.458	0.449	0.019	0.028	0.000361	0.000784
50	0.45	0.392	0.384	0.058	0.066	0.003364	0.004356
Mean Square Error						0.0112	0.0099

The Mean Square Error of the Uncompensated Cup-to-Disk Ratio is 0.0112, while this error for Cup-to-Disk Ratio compensated by factor of 0.98 is 0.0099. We see a reduction in 13% of mean square error. Moreover there is no change in the diagnostic accuracy.

Table 6.7: Comparison of Compensated CDR values with **α=** 0.97

S. no.	CDR (True)	CDR (Measured)	CDR (Compensated) = CDR (Measured)*0.97	Uncompensated Error= CDR (True – Measured)	Compensated Error= CDR (True-Compensated)	Uncompensated Error Square	Compensated Error Square
1	0.427	0.408	0.396	0.019	0.031	0.000	0.001
2	0.553	0.567	0.55	-0.014	0.003	0.000	0.000
3	0.433	0.482	0.468	-0.049	-0.035	0.002	0.001
4	0.538	0.603	0.585	-0.065	-0.047	0.004	0.002
5	0.626	0.825	0.8	-0.199	-0.174	0.040	0.030
6	0.402	0.333	0.323	0.069	0.079	0.005	0.006
7	0.365	0.472	0.458	-0.107	-0.093	0.011	0.009
8	0.63	0.873	0.847	-0.243	-0.217	0.059	0.047
9	0.576	0.731	0.709	-0.155	-0.133	0.024	0.018
10	0.451	0.485	0.47	-0.034	-0.019	0.001	0.000
11	0.484	0.398	0.386	0.086	0.098	0.007	0.010
12	0.562	0.575	0.558	-0.013	0.004	0.000	0.000
14	0.483	0.474	0.46	0.009	0.023	0.000	0.001
16	0.402	0.472	0.458	-0.07	-0.056	0.005	0.003
18	0.66	0.825	0.8	-0.165	-0.14	0.027	0.020
19	0.404	0.308	0.299	0.096	0.105	0.009	0.011
22	0.421	0.271	0.263	0.15	0.158	0.023	0.025
24	0.373	0.321	0.311	0.052	0.062	0.003	0.004
26	0.471	0.574	0.557	-0.103	-0.086	0.011	0.007
27	0.403	0.508	0.493	-0.105	-0.09	0.011	0.008
28	0.441	0.433	0.42	0.008	0.021	0.000	0.000
29	0.661	0.886	0.859	-0.225	-0.198	0.051	0.039
30	0.371	0.305	0.296	0.066	0.075	0.004	0.006
31	0.37	0.28	0.272	0.09	0.098	0.008	0.010
33	0.377	0.417	0.404	-0.04	-0.027	0.002	0.001
34	0.337	0.272	0.264	0.065	0.073	0.004	0.005
35	0.624	0.724	0.702	-0.1	-0.078	0.010	0.006
36	0.576	0.607	0.589	-0.031	-0.013	0.001	0.000
37	0.5	0.5	0.485	0	0.015	0.000	0.000
38	0.468	0.695	0.674	-0.227	-0.206	0.052	0.042

S. no.	CDR (True)	CDR (Measured)	CDR (Compensated) = CDR (Measured)*0.97	Uncompensated Error= CDR (True – Measured)	Compensated Error= CDR (True-Compensated)	Uncompensated Error Square	Compensated Error Square
39	0.68	0.82	0.795	-0.14	-0.115	0.020	0.013
41	0.598	0.679	0.659	-0.081	-0.061	0.007	0.004
42	0.754	0.763	0.74	-0.009	0.014	0.000	0.000
44	0.571	0.656	0.636	-0.085	-0.065	0.007	0.004
45	0.53	0.66	0.64	-0.13	-0.11	0.017	0.012
46	0.616	0.515	0.5	0.101	0.116	0.010	0.013
47	0.423	0.404	0.392	0.019	0.031	0.000	0.001
48	0.421	0.515	0.5	-0.094	-0.079	0.009	0.006
49	0.477	0.458	0.444	0.019	0.033	0.000	0.001
50	0.45	0.392	0.38	0.058	0.07	0.003	0.005
Mean Square Error						0.0112	0.0093

The Mean Square Error for the Uncompensated Cup-to-Disk Ratio is 0.0112, while this error is 0.0093 for the CDR compensated by factor of 0.97. Here, we see a reduction in 20% of mean square error.

However the use of 0.97 as a compensation factor increases the False Negative in diagnosis i.e. it identifies a Glaucomatous sample as normal (highlighted in Table 6.7, sample no. 46) and hence is not recommended. 0.98 is thus justified as the suitable compensation factor for the normalization of CDR values.

CHAPTER 7
CONCLUSIONS AND FUTURE SCOPE

7.1 Conclusion

Glaucoma is a serious eye disorder that affects optic nerve. One way to screen the subjects for Glaucoma is by measuring the Cup-to-Disc Ratio of the Retinal Fundus Images. In this dissertation, 50 image samples have been acquired and worked upon. The samples are processed using Image Processing Toolbar in MATLAB. The Optic Disc and Cup of 40 out of 50 image samples have been detected. The Cup-to-disc Ratios of these 40 samples have been calculated accordingly. The measured CDRs have been compared with the gold standard values and 38 out of the detected 40 samples are detected correctly. The proposed algorithm achieved CDR detection rate of 80% and a classification accuracy of 95% of the detected images, sensitivity and specificity of 100% and 91%. The Cup-to-disc Ratio values calculated for normal samples lies in the range of 0.3 to 0.5 while it is greater than 0.5 for the samples suspicious for Glaucoma. The Mean of the normal CDR values comes out to be 0.40 and for the suspicious samples it is observed as 0.65

The study and work that has been carried out in this dissertation provides a simple algorithm for the screening of the disease Glaucoma. The higher eye pressure indicates a pathological condition but sometimes a certain level of eye pressure may be high for one but normal for another. Once the images are screened using the CDR values, it removes the ambiguity by classifying the samples as normal or suspicious for Glaucoma and further work can be carried out for the confirmation of the disease.

7.2 Future Scope

This dissertation proposed a methodology to screen the samples for Glaucoma. The future scope for this research can be the extraction of further features that can provide a confirmatory result i.e. classify the sample as Glaucomatous or Normal. The presence of Glaucoma, after screening by the CDR values, can be confirmed by the evaluation of the ISNT Quadrants and the Neuro-Retinal Rim Area (NRRA). The proposed algorithm achieved a detection rate of 80% which can be further enhanced by using higher number of samples.

REFERENCES

[1] M. Singh, Introduction to Biomedical Instrumentation, PHI Learning Pvt. Ltd., 2010, PP: 5-6.

[2] Rhee, Douglas J. (August 2013). Porter, Robert S.; Kaplan, Justin L., eds."Glaucoma". The Merck Manual Home Health Handbook. Retrieved December 12, 2013.

[3] Damage to Optic Nerve due to Increased Eye pressure, Available at: http://en.dunyagoz.com/treatments/glaucoma-high-eye-pressure.html?print=1

[4] Aqueous Fluid Pathway, available at: http://www.naturaleyecare.com/ocular-support/optic-nerve-support/intraocular-pressure.asp.

[5] Glaucoma and your eyes, Available at: http://www.webmd.com/eye-health/glaucoma-eyes

[6] Glaucoma: Causes, Risk Factors, Symptoms, Diagnosis and Treatment, Available at:http://www.southernophthalmology.com.au/glaucoma.html#glaucoma

[7] Normal Fundus, Available at: http://homedesignblogs.net/tag/fundus-definition-of-fundus-by-medical-dictionary

[8] Healthy and Unhealthy Optic Disk, Available at: http://galleryhip.com/open-angle-glaucoma-cup-to-disc-ratio.html.

[9] ISNT Quadrants, Available at: http://www.ijo.in/article.asp?issn.

[10] H. Li, O. Chutatape, "A Model-Based Approach for Automated Feature Extraction in Fundus Images", *Computer Vision Proceedings. Ninth IEEE International Conference,* pp. 394 - 399 Vol.1, 2003.

[11] J. Lowell, A. Hunter, D. Steel, A. Basu, R. Ryder, E. Fletcher, and L. Kennedy, "Optic nerve head segmentation", *IEEE Transactions on Medical Imaging* , Vol 23, pp. 256 – 264.

[12] K. Noronha, J. Nayak, S. N. Bhatt, "Enhancement of retinal fundus image to highlight the features for detection of abnormal eyes", *10th Conference in IEEE*, pp. 1- 4, 2004.

[13] A. A. Haleim, A. R. Youssif, A. Z. Ghalwash, and A. A. Sabry A. R. Ghoneim, "Optic Disc Detection From Normalized Digital Fundus Images By Means Of A Vessels‟

Direction Matched Filter", *IEEE Transactions On Medical Imaging*, Vol 27 Issue 1, pp. 11-18, 2008.

[14] J. Liu1, D. W. K. Wong1, J.H. Lim1, X. Jia1, F. Yin1, H. Li1, W. Xiong1, T. Y. Wong2, "Optic Cup and Disk Extraction from Retinal Fundus Images For Determination Of Cup-To-Disc Ratio", *IEEE Conference on Industrial Electronics and Applications*, 2008.

[15] S. Sekhar, W. A. Nuaimy and A. K. Nandi "Automated Localisation Of Retinal Optic Disk Using Hough Transform", *Biomedical Imaging: From Nano to Macro*, 2008, 978-1-4244-2002-5, pp. 1577-1580, 2008.

[16] Radim Kolář, "Detection Of Glaucomatous Eye Via Color Fundus Images Using Fractal Dimensions", *Radio Engineering*, Vol 17 Issue 3, 2008.

[17] G. B. Kande, P. V. Subbaiah, T. S. Savithri, "Feature Extraction in Digital Fundus Images", *Journal of Medical and Biological Engineering*, Vol 29, Issue 3, pp. 122-130, 2009.

[18] X. Zhu, R. M Ranggayyan, "Detection of the optic disc in images of retina using Hough transform", *Conference Proceedings IEEE Engineering Medical Biological Society*, pp. 3456 – 3459, 2008.

[19] G. B. Kande, P. V. Subbaih, and T. Satya Savithri, "Segmentation of exudates and optic disc in retinal images", *6th Indian Conference on Computer Vision, Graphics and Image Processing*, pp. 535 – 540, 2008.

[20] A.W. Reza, C. Eswaran, S. Hati " Automatic Tracing Of Optic Disc And Exudates From Color Fundus Images Using Fixed And Variable Thresholds", *Journal of Medical Systems*, Vol. 33, Issue. 1, pp. 73-80, 2009.

[21] J. Nayak, R. Acharya, U. P. S. Bhat, N. Shetty, T. C. Lim, "Automated Diagnosis of Glaucoma Using Digital Fundus Images", Volume 33 Issue 5, pp. 337 – 346, 2009.

[22] S. Ravishankar, A. Jain, and A. Mittal, "Automated feature extraction of early detection of diabetic retinopathy in fundus images", *International Conference in IEEE*, pp 210-220, 2009.

[23] R. Bock, J. Meier, G. Michelson, L. G. Ny´ul1 and J. Hornegger "Classifying Glaucoma With Image-Based Features From Fundus Photographs", *Pattern Recognition Lecture Notes in Computer Science*, Vol 14 Issue 3, pp. 471-481, 2010.

[24] R. Bock, J. Meier, L. G. Nyúl , J. Hornegger , G. Michelson, "Glaucoma risk index: Automated glaucoma detection from color fundus images", *Medical Image Analysis*, Vol 14, pp. 471–481, 2010.

[25] C. Muramatsua, T. Nakagawab, A. Sawadac, Y. Hatanakad, T. Haraa, T. Yamamotoc, H. Fujitaa, "Automated Segmentation Of Optic Disc Region On Retinal Fundus Photographs: Comparison Of Contour Modeling And Pixel Classification Methods", *Computer methods and programs in biomedicine*, Vol 101 Issue 1, pp. 23-32, 2010.

[26] A. Aquino, M. E. G. Arias, and D. Marín, "Detecting The Optic Disc Boundary In Digital Fundus Images Using Morphological, Edge Detection, And Feature Extraction Techniques", *IEEE Transactions On Medical Imaging*, Vol 29 Issue 11, pp. 1860-1869, 2010.

[27] D. W. K. Kong, J. Liu, N. M. Tan, F. Yin, B. H. Lee, and T. Y. Wong, "Learning based approach for the automatic detection of the optic disc in retinal fundus photograph", *32nd Annual International Conference of the IEEE*, pp. 5355 – 5358, 2010.

[28] E. Mahfouz, and A. S. Fahmy," Fast Localization of the optic disc using projection of image features", *IEEE Transactions on Image Proceedings*, Vol 19, pp. 3285 – 3289, 2010.

[29] P. C. Siddalingaswamy, and K. G. Prabhu, "Automated grading of diabetic maculopathy severity levels", *Proceedings of International Conference on Systems in Medicine and Biology*, pp. 331 – 334, 2010.

[30] M. Mishra, M. K. Nath and S. Dandapat, "Glaucoma Detection From Color Fundus Images", *International Journal of Computer & Communication Technology*, Vol 2 Issue 6, 2011.

[31] A.W. Reza, C. Eswaran, S. Hati " Automatic Tracing Of Optic Disc And Exudates From Color Fundus Images Using Fixed And Variable Thresholds", *Journal of Medical Systems*, Vol. 33, Issue 1, pp. 73-80, 2009.

[32] F. Yin, J. Liu, S. H. Ong, Y. Sun, Damon W. K. Wong, N. M. Tan, C. Cheung, M. Baskaran, T. Aung, T. Y. Wong, "Model based optic nerve head segmentation on retinal fundus images", *33rd Annual International Conference of the IEEE*, pp. 2626 – 2629, 2011.

[33] J. Cheng, J. Liu, D. W. K. Wong, F. Yin, C. Cheung, M. Baskaran, T. Aung, and T. Y. Wong, "Automatic optic disc segmentation with peripapillary atrophy elimination", *33rd International Conference of the IEEE*, pp. 6224 – 6227, 2011.

[34] Dehgani, H. A. Moghaddam, M. S. Moin, "Optic disc localization in retinal images using histogram matching", *Journal on Image and Video Processing*, pp. 2012 – 2019, 2012.

[35] M. Esameili, H. Rabbani, A. M. Dehnavi, and A. Dehghani , " Automatic detection of exudates and optic disk in retinal images using curvelet transform", *IET Image Process*, Vol 6, pp. 1005 – 1013, 2012.

[36] S.Kavitha , K.Duraiswamy, "An Efficient Decision Support System Detection Of Glaucoma In Fundus Images Using Anfis", *International Journal Of Advances In Engineering & Technology*, Vol. 2, Issue 1, pp. 227-240, 2012.

[37] H. Yu, E. S. Barriga, C. Agurto, S. Echegaray, M. S. Pattichis, W. Bauman, and P. Soliz, "Fast localization and segmentation of optic disc in retinal images using directional matched filtering and level sets", *IEEE Transactions on Information Technology in Biomedicine*, Vol 16, pp 644 – 657, 2012.

[38] M.H.S.P. Kumara and R. G. N. Meegama. "Active contour-based segmentation and removal of optic disk from retinal images", *In Advances in ICT for Emerging Regions (ICTer), 2013 International Conference*, pp. 15-20, 2013.

[39] F. Khan, S. A. Khan, U. U. Yasin, I. ul Haq, U. Qamar, "Detection of Glaucoma Using Retinal Fundus Images", *The 2013 Biomedical Engineering International Conference*, 2013.

[40] Preeti, J. Pruthi, "Review Of Image Processing Technique For Glaucoma Detection", *International Journal Of Computer Science And Mobile Computing*, Vol 2 Issue 11, pp. 99-105, 2013.

[41] J. Cheng, J. Liu, Y. Xu, F. Yin, Damon Wing Kee Wong, N. M. Tan, D. Tao, C.Y. Cheng, T. Aung, and T. Y. Wong ," Super pixel classification based optic disc and optic cup segmentation for glaucoma screening", *IEEE Transactions on Medical Imaging*, Vol 32, pp. 1019 – 1032, 2013.

[42] S. Gonzalez, D. Kaba, Y. Li and X. Liu, "Segmentation of blood vessels and optic disc in retinal images", *IEEE Journal of Biomedical and Health Informatics*, pp. 1-14, 2014.

[43] http://www.geteyesmart.org/eyesmart/diseases/glaucoma/

[44] Optic Nerve Damage due to elevated pressure, Available at: https://www.healthtap.com/topics/optic-cupping.

[45] Powers, David M W, "Evaluation: From Precision, Recall and F-Measure to ROC, Informedness, Markedness & Correlation" (PDF). *Journal of Machine Learning Technologies*, Vol **2**, Issue 1, pp. 37–63, 2011.

[46] http://www.socialresearchmethods.net/kb/stat_t.php.